Applied Mathematics and Computation 507 (2025) 129599

Contents lists available at ScienceDirect

Applied Mathematics and Computation

journal homepage: www.elsevier.com/locate/amc

Full Length Article

A unified model of SABR and mean-reverting stochastic volatility for derivative pricing

Sun-Yong Choi [a], Jeong-Hoon Kim [b,*]

[a] Department of Finance and Big Data, Gachon University, Seongnam, Gyeonggi 13120, Republic of Korea
[b] Department of Mathematics, Yonsei University, Seoul 03722, Republic of Korea

ARTICLE INFO

JEL classification:
G13
G12

MSC:
91G20
91G15
35B20
60H10

Keywords:
SABR
Mean-reversion
Multiscale
Stochastic-local volatility
Asymptotics
Mellin transform

ABSTRACT

The SABR model is popularly used by practitioners in the financial industry due to a fairly simple implied volatility formula but it wouldn't capture the mean reverting nature of the volatility as a drawback. This paper proposes a stochastic-local volatility model that unifies SABR volatility and mean reverting stochastic volatility for pricing derivatives. We obtain an explicit pricing formula in convolution form through the combination of asymptotics and the Mellin transform method. The formula allows us to compute the derivative price in terms of a single integral calculation (Mellin convolution) instead of a double integral. Further, we obtain a closed-form pricing formula that can be calculated by using the three Greeks (Delta, Gamma, and Speed) of the Black-Scholes derivative price in a reasonably practical situation. The accuracy of the derived formula is tested through Monte Carlo simulation. The validity of the formula is demonstrated through an empirical analysis of a foreign exchange option, as incorporating a mean-reverting volatility feature into the SABR model aids in calibrating the model to real market instruments by reproducing the U-shaped structure of the implied volatility.

1. Introduction

The SABR model is one of the stochastic-local volatility models popularly used by practitioners, especially in the interest rate derivative and foreign exchange markets, in an attempt to capture the volatility smile. The name stands for "stochastic α (alpha), β (beta), ρ (rho)", referring to the parameters of the stochastic differential equations (SDEs)

$$\begin{aligned} dS_t &= X_t S_t^{\beta}\, dW_t^s, \\ dX_t &= \alpha X_t\, dW_t^x, \;\; d\langle W^s, W^x\rangle_t = \rho\, dt \end{aligned} \tag{1.1}$$

which was developed by Hagan et al. [1], where W_t^s and W_t^x are standard Brownian motions and α (vol-of-vol), β (skewness) and ρ (correlation between the underlying and its volatility) are assumed to satisfy $\alpha > 0$, $\beta > 0$ and $-1 < \rho < 1$, respectively. Given the underlying of a considered derivative, X_t controls the volatility level of the underlying. In particular, the initial volatility X_0 controls the height of the ATM implied volatility level. The volatility of volatility α controls the implied volatility curvature while both β

* Corresponding author.
E-mail addresses: sunyongchoi@gachon.ac.kr (S.-Y. Choi), jhkim96@yonsei.ac.kr (J.-H. Kim).

https://doi.org/10.1016/j.amc.2025.129599
Received 12 July 2024; Received in revised form 29 May 2025; Accepted 4 June 2025

and ρ control the slope of the implied volatility skew. The parameter β is often fixed before the calibration of the other parameters (cf. West [2]) because of the similar effect on the skew. There is no exact closed-form solution for the probability distribution of the process S_t but there is an asymptotic solution in the small parameter $T\alpha^2$ in terms of implied volatility, where T is the time to expiration of a European option.

There are variants and extensions of the SABR model due to the unrealistic assumption that the variance process X_t in (1.1) is a geometric Brownian motion. One of them is the '$\lambda-$ SABR model' of Henry-Labordère [3] in which a mean-reverting drift term is integrated in the SDE for X_t. By replacing S_t^β with $|S_t|^\beta$ in (1.1), Antonov et al. [4] considered the 'free boundary SABR model' not bounding how negative interest rates can become. In addition, the standard SABR model can be extended by making the parameters time-dependent, as studied by Van Der Stoep et al. [5] and Guerrero and Orlando [6]. Cui et al. [7] considered a general stochastic-local volatility framework that covers the SABR model and some of its variants.

The SABR model is reduced to the CEV model that Cox introduced [8] when α merges to 0. So, it is a stochastic generalization of the CEV model with the skewness parameter β. The parameter β is the central feature of the CEV model and controls the relationship between the underlying price and its volatility. We commonly observe $\beta < 1$ (the leverage effect) in equity markets (cf. Yu [9] for example), while $\beta > 1$ (the inverse leverage effect) in commodity markets (cf. Geman and Shih [10] for example). The special case $\beta = 1$ becomes the geometric Brownian motion as in the Black-Scholes model [11]. Another stochastic generalization of the CEV model is the so-called SVCEV model developed by Choi et al. [12] based on the observation that volatility will eventually return to the long-run mean or average level of the entire dataset (cf. Fouque et al. [13] for example). So, it is similar to the $\lambda-$ SABR model, but the geometric Brownian motion X_t in the SABR model is replaced by a mean-reverting Ornstein-Uhlenbeck process. In particular, the mean reversion rate is high enough to apply the averaging theory developed by Fouque et al. [14] and obtain an asymptotic solution with a leading-order term given by the CEV formula for European derivatives. Here, the averaging theory could be understood as an asymptotic expansion with the leading-order and first correction terms obtained by the Law of Large Numbers and the Central Limit Theorem, respectively. This is related to the asymptotic diffusion limit theory with a small parameter studied by Khasminskii [15], Papanicolaou and Kohler [16], Cerrai [17], and Bao et al. [18].

This paper blends the SABR volatility and the SVCEV volatility so that the SABR volatility is equipped with a mean reversion property in the unified model. Volatility is recognized as mean reverting in many derivative-pricing models, as this feature aids in calibrating the model to real-market instruments. The volatility means reversion property was observed in an empirical analysis of high-frequency S&P 500 index data as shown by Fouque et al. [13], which confirms that volatility reverts slowly to its mean compared to tick-by-tick fluctuations of the S&P 500 index value, but it is a fast mean reverting when looked at over the time scale of a derivative contract. Bali and Demirtas [19] found empirical evidence indicating that conditional variance, log-variance, and standard deviation of S&P 500 index futures returns are pulled back to some long-term average level over time. On the other hand, Lee [20] used a mean reverting volatility framework to model commodity price dynamics and developed a generic procedure for model calibration. In general, it is very difficult to find a derivative price formula explicitly under a stochastic-local volatility model, resulting in the loss of some analytic tractability. Even if a solution formula is obtained for the derivative price, double integration is required to calculate the formula in most cases. However, since the SABR and SVCEV models provide explicit asymptotic solution formulas, we are able to obtain an easy-to-compute valuation formula for European derivatives under the unified SABR and SVCEV model. The formula is expressed in convolution form, so only one integration is required to calculate the formula. As a subsequent result of the formula, we obtain a closed-form pricing formula that can be calculated by taking a certain combination of the Greeks (Delta, Gamma, and Speed) of the Black-Scholes derivative price under a practically reasonable assumption for the elasticity of variance. This is a very useful result from a computational point of view. We provide two specific examples (European vanilla option and variance swap) of calculating the derivative price based on the formula. Another advantage of our formula is that an alternative expression of the known pricing formula under some local or stochastic volatility model can be reproduced in reduced form. We verify the validity of the unified formula through an empirical analysis of foreign exchange options. In particular, the U-shaped structure of the implied volatility can be approximated by our result.

The remainder of the paper is organized as follows. In Section 2, we write the unified model of the SABR and SVCEV volatilities. In Section 3, we derive an asymptotic pricing formula for European derivatives in terms of Mellin convolution. In addition, we obtain an approximate closed-form expression near zero elasticity of variance (in terms of the Black-Scholes price). Section 4 provides two specific cases, European vanilla option and variance swap, as an application of our pricing formula. In Section 5, we demonstrate the performance of the proposed model in real-world scenarios in terms of implied volatility using the GBP/USD options. Finally, we give some concluding remarks in Appendix A.

2. Model and derivative pricing

2.1. Model

In this paper, we introduce a new stochastic-local volatility model that blends SABR volatility with SVCEV volatility. Since the SABR pricing formula is available under the condition that $T\alpha^2$ is small, we change the original notation α in the SABR model (1.1) to a small parameter $\sqrt{\delta}$. In addition, we use the notation θ instead of β. Then our model for the price dynamics of risky assets is given by

Table 1
Reduced models depending on the specification of the model parameters θ, ϵ and δ. Here, SV_f stands for stochastic volatility of fast variation, and MSV and CEV are the initials of multiscale stochastic volatility and constant elasticity of variance, respectively.

Parameter specification : Reduced models	
$1-\theta, \epsilon, \delta \to 0$: Black-Scholes	$\epsilon, \delta \to 0$: CEV
$1-\theta, \delta \to 0$: SV_f	$1-\theta \to 0$: MSV
$\epsilon \to 0$: SABR	$\delta \to 0$: SVCEV

$$\begin{aligned} dS_t &= \left(X_t + f(Y_t)\right) S_t^{\theta}\, dW_t^s, \\ dX_t &= \sqrt{\delta}\, X_t\, dW_t^x, \\ dY_t &= \frac{1}{\epsilon}\,\alpha(Y_t)\, dt + \frac{1}{\sqrt{\epsilon}}\,\beta(Y_t)\, dW_t^y, \end{aligned} \tag{2.1}$$

where θ, ϵ and δ are real numbers satisfying $0<\theta<1$ and $0<\delta,\epsilon\ll 1$. W^s, W^x and W^y are Brownian motions defined on a filtered probability space $(\Omega,\mathcal{F},\mathcal{F}_t,\mathbb{Q})$ and they have a correlation structure expressed as

$$d\langle W^s, W^x\rangle_t = \rho_{sx}dt,\ \ d\langle W^s, W^y\rangle_t = \rho_{sy}dt,\ \ d\langle W^x, W^y\rangle_t = \rho_{xy}dt.$$

The functions f and α and β are assumed to satisfy the smooth and boundedness conditions necessary for the stochastic differential equation for S_t to have a unique solution. The time horizon is restricted to the interval $[0,\tau)$ where $\tau := \min\{t>0 : S_t = 0\}$. In this paper, the process Y_t is chosen to be ergodic (mean-reverting) and to have an invariant distribution denoted by Φ so that the averaging theory of Fouque et al. [14] can be applied. Y_t can be, for example, the Ornstein-Uhlenbeck process defined by $\alpha(y)=m-y$ and $\beta(y)=\sigma$ and the CIR process defined by $\alpha(y)=m-y$ and $\beta(y)=\sigma\sqrt{y}$ for some positive constants m and σ. Throughout the paper, we frequently use the notation

$$\langle g(\cdot)\rangle := \int g(y)\,\Phi(y)\,dy \tag{2.2}$$

for the average of the function g with respect to the invariant distribution Φ. We call (2.1) the unified model or the SABR-SVCEV model.

There are two small parameters in the unified model (2.1). The small parameter δ suggests that the SABR approximation formula for implied volatility is still expected to be available even if the time to maturity is not that short. On the other hand, the small parameter ϵ implies that the volatility process is speeded up by rescaling time t in terms of ϵ. The empirical reason for this participation is that volatility is fast mean reverting on the time scale of a derivative contract, which was confirmed by the study by Fouque et al. [13] based on an analysis of high-frequency S&P 500 index data. The fast mean reverting volatility method has also been used for interest rate derivatives to produce a better fit of the yield curve (Cotton et al. [21], for example) and portfolio optimization to accurately estimate the distribution of the loss from a large portfolio (Hambly and Kolliopoulos [22], for example). However, technically, the small parameter ϵ plays a role in the application of the averaging principle to the derivation of a derivative price formula. The volatilities are sped up towards a limiting distribution so that asymptotic expansion with a few numbers of terms such as the leading order and first correction terms would be a reasonable approximation for the derivative price. Here, the leading-order and first correction terms can be thought of as the results of the Law of Large Numbers and the Central Limit Theorem in discrete probability language when $1/\epsilon$ is replaced by the natural number n. The idea has a long history that can be traced back to the original work of Khasminskii [15] for stochastic differential equations with a small parameter.

One can notice that if some of the parameters in the model (2.1) vanish, then previously known models can be recovered. For example, if $\delta\to 0$, then the model is reduced to the SVCEV model. If $\epsilon\to 0$, then it becomes the SABR model. If $\theta\to 1$ and $\epsilon,\delta\to 0$, then it converges to the Black-Sholes model. See the reduced models listed in Table 1.

2.2. Derivative price formula

From the Feynman-Kac theorem (cf. Karatzas and Shreve [23]), the derivative price $P^{\epsilon,\delta}(t,s,x,y)$, defined by the conditional expectation

$$P^{\epsilon,\delta}(t,s,x,y) = E^{\mathbb{Q}}[h(S_T)\,|\,S_t=s, X_t=x, Y_t=y] \tag{2.3}$$

under a risk-neutral probability measure $\mathbb{Q}$, satisfies a final value problem expressed by

$$\begin{aligned} &\mathcal{L}^{\epsilon,\delta} P^{\epsilon,\delta}(t,s,x,y) = 0, \quad 0\le t<T, \\ &P^{\epsilon,\delta}(T,s,x,y) = h(s), \end{aligned} \tag{2.4}$$

where h is the payoff of the considered derivative and $\mathcal{L}^{\epsilon,\delta}$ is a multiscale differential operator given by

$$
\begin{aligned}
\mathcal{L}^{\epsilon,\delta} &= \frac{1}{\epsilon}\mathcal{L}_0 + \frac{1}{\sqrt{\epsilon}}\mathcal{L}_1 + \mathcal{L}_2 + \sqrt{\frac{\delta}{\epsilon}}\mathcal{M}_3 + \sqrt{\delta}\mathcal{M}_1 + \delta\mathcal{M}_2,\\
\mathcal{L}_0 &:= \alpha(y)\,\partial_y + \frac{1}{2}\beta^2(y)\,\partial_{yy},\\
\mathcal{L}_1 &:= \rho_{sy}\,(x+f(y))\,\beta(y)\,\mathcal{D}_{\theta,1}\partial_y,\\
\mathcal{L}_2 &:= \partial_t + \frac{1}{2}\,(x+f(y))^2\mathcal{D}_{2\theta,2},\\
\mathcal{M}_1 &:= \rho_{sx}\,(x+f(y))\,\mathcal{D}_{\theta,1}\mathcal{D}^x_{1,1},\\
\mathcal{M}_2 &:= \frac{1}{2}\mathcal{D}^x_{2,2},\\
\mathcal{M}_3 &:= \rho_{xy}\,\beta(y)\,\mathcal{D}^x_{1,1}\partial_y,
\end{aligned}
\tag{2.5}
$$

where

$$
\mathcal{D}_{m,n} := s^m\partial_{s^n}, \quad \mathcal{D}^x_{m,n} := x^m\partial_{x^n}. \tag{2.6}
$$

Since the PDE problem (2.4) is a singular perturbation problem, we are interested in an asymptotic solution of the form

$$
P^{\epsilon,\delta}(t,s,x,y) = \sum_{i,j=0}^{\infty} (\sqrt{\delta})^i(\sqrt{\epsilon})^j\, P_{ij}(t,s,x,y). \tag{2.7}
$$

In particular, our goal is to obtain the leading order and the first correction terms in δ and ϵ. Speaking about an expansion with respect to ϵ, the leading term P_{i0} is the value given under the SABR model, and the first correction term P_{i1} can be thought of as a result of the Central Limit Theorem (when ϵ is replaced by $1/n$).

Following the multiscale asymptotic analysis of Fouque et al. [14] and using the operator $\mathcal{L}_{\text{CEV}}$ defined by

$$
\begin{aligned}
\mathcal{L}_{\text{CEV}} &= \partial_t + \frac{1}{2}\,\bar{\sigma}_f^2(x)\,\mathcal{D}_{2\theta,2},\\
\bar{\sigma}_f(x) &:= \sqrt{\langle (x+f(\cdot))^2\rangle},
\end{aligned}
\tag{2.8}
$$

one can prove that first, P_{00}, P_{01}, and P_{10} are independent of the variable y and second, they satisfy the PDE problems

$$
\begin{aligned}
&\mathcal{L}_{\text{CEV}}P_{00}(t,s,x) = \langle\mathcal{L}_2\rangle P_{00} = 0, \quad P_{00}(T,s,x) = h(s),\\
&\mathcal{L}_{\text{CEV}}P_{01}(t,s,x) = \langle\mathcal{L}_1\mathcal{L}_0^{-1}(\mathcal{L}_2 - \langle\mathcal{L}_2\rangle)\rangle P_{00} = A_{01}(x)\mathcal{D}_{\theta,1}\mathcal{D}_{2\theta,2}P_{00}(t,s,x), \quad P_{01}(T,s,x) = 0,\\
&\mathcal{L}_{\text{CEV}}P_{10}(t,s,x) = -\langle\mathcal{M}_1\rangle P_{00} = -A_{10}(x)\mathcal{D}_{\theta,1}\mathcal{D}^x_{1,1}P_{00}(t,s,x), \quad P_{10}(T,s,x) = 0,
\end{aligned}
\tag{2.9}
$$

respectively, where the functions $A_{01}(x)$ and $A_{10}(x)$ are

$$
\begin{aligned}
A_{01}(x) &:= \frac{1}{2}\rho_{sy}\langle (x+f(\cdot))\beta(\cdot)\partial_y\phi(x,\cdot)\rangle,\\
A_{10}(x) &:= \rho_{sx}(x+\langle f(\cdot)\rangle),
\end{aligned}
\tag{2.10}
$$

respectively. Here, $\phi(x,y)$ is a function defined by solution to

$$
\mathcal{L}_0\phi(x,y) = (x+f(y))^2 - \langle (x+f(\cdot))^2\rangle. \tag{2.11}
$$

Note that $A_{01}(x)$ is related to the fast mean reverting variation of volatility, while $A_{10}(x)$ is connected with the slow-scale variation of the SABR type of volatility. We leave the proof of y independence of the terms P_{00}, P_{01} and P_{10} and the derivation of the PDEs in (2.9) to **Appendix**.

Since $\mathcal{L}_{\text{CEV}}$ defined by (2.8) is the differential operator ∂_t plus the infinitesimal generator of the CEV diffusion solving the stochastic differential equation

$$
dS_t = \bar{\sigma}_f(x)\,S_t^{\theta}\,dW_t^s \tag{2.12}
$$

as its notation suggests, the PDE problem $\mathcal{L}_{\text{CEV}}P_{00}(t,s,x) = 0$ with the final condition $P_{00}(T,s,x) = h(s)$ gives us that P_{00} is the CEV derivative price and subsequently we use notation P_{CEV} instead of P_{00} from now on. There is a closed-form probability density function available to solve the CEV diffusion (2.12). It is given by

$$
\begin{aligned}
p(t,s;\tilde{t},\tilde{s}) &= 2(1-\theta)k^{\frac{1}{2(1-\theta)}}(uv^{1-2\theta})^{\frac{1}{4(1-\theta)}}\,e^{u-v}\,I_{1/2(1-\theta)}(2\sqrt{uv}),\\
k &:= \frac{1}{2\bar{\sigma}_f^2(1-\theta)^2(\tilde{t}-t)},\\
u &:= ks^{2(1-\theta)},\\
v &:= k\tilde{s}^{2(1-\theta)},
\end{aligned}
\tag{2.13}
$$

where $I_q(x)$ is the modified Bessel function of the first kind of order q. From the Feynman-Kac theorem, P_{01} and P_{10} solving the PDEs in (2.9) are given by

$$\begin{aligned} P_{01}(t,s,x) &= E^{\mathbb{Q}}\left[-\int_t^T A_{01}(x)\mathcal{D}_{\theta,1}\mathcal{D}_{2\theta,2}P_{\mathrm{CEV}}(\tilde{t},S_{\tilde{t}},x)\,d\tilde{t}\mid S_t=s\right] \\ &= -A_{01}(x)\int_0^\infty\int_t^T p(t,s;\tilde{t},\tilde{s})\,\mathcal{D}_{\theta,1}\mathcal{D}_{2\theta,2}P_{\mathrm{CEV}}(\tilde{t},\tilde{s},x)\,d\tilde{t}\,d\tilde{s}, \\ P_{10}(t,s,x) &= E^{\mathbb{Q}}\left[\int_t^T A_{10}(x)\mathcal{D}_{\theta,1}\mathcal{D}^x_{1,1}P_{\mathrm{CEV}}(\tilde{t},S_{\tilde{t}},x)\,d\tilde{t}\mid S_t=s\right] \\ &= A_{10}(x)\int_0^\infty\int_t^T p(t,s;\tilde{t},\tilde{s})\,\mathcal{D}_{\theta,1}\mathcal{D}^x_{1,1}P_{\mathrm{CEV}}(\tilde{t},\tilde{s},x)\,d\tilde{t}\,d\tilde{s}, \end{aligned} \tag{2.14}$$

respectively, in term of the probability density function $p(t,s;\tilde{t},\tilde{s})$ given in (2.13). However, it seems better to use the Mellin transform to express the solutions for P_{01} and P_{10}. The transform can lead to a single integral (instead of double integral) expression of each of these terms as shown below.

To solve the PDE problems in (2.9) for P_{01} and P_{10}, we use Mellin transform and its inverse transform defined by

$$(\mathcal{M}g)(\omega) := \hat{g}(\omega) = \int_0^\infty g(s)\,s^{\omega-1}\,ds, \quad (\mathcal{M}^{-1}\hat{g})(s) := g(s) = \frac{1}{2\pi i}\int_{a-i\infty}^{a+i\infty}\hat{g}(\omega)\,s^{-\omega}\,d\omega,$$

respectively, for a real number a under the condition given in the Mellin inversion theorem (cf. Debonath and Bhatta [24]). Taking the Mellin transform of (2.9), we obtain the ODE problems for $\hat{P}_{00}$, $\hat{P}_{01}$ and $\hat{P}_{10}$ as follows.

$$\begin{aligned} &\partial_t\hat{P}_{\mathrm{CEV}}(t,\omega,x)+\lambda(\omega,x)\hat{P}_{\mathrm{CEV}}(t,\omega,x)=0, \quad \hat{P}_{\mathrm{CEV}}(T,\omega,x)=\hat{h}(\omega), \\ &\partial_t\hat{P}_{01}(t,\omega,x)+\lambda(\omega,x)\hat{P}_{01}(t,\omega,x)=g_{01}(t,\omega,x), \quad \hat{P}_{01}(T,\omega,x)=0, \\ &\partial_t\hat{P}_{10}(t,\omega,x)+\lambda(\omega,x)\hat{P}_{10}(t,\omega,x)=g_{10}(t,\omega,x), \quad \hat{P}_{10}(T,\omega,x)=0, \end{aligned} \tag{2.15}$$

where $\hat{h}(\omega)$ is the Mellin transform of $h(s)$ and the functions $\lambda(\omega,x)$, $g_{01}(t,\omega,x)$ and $g_{10}(t,\omega,x)$ are

$$\begin{aligned} \lambda(\omega,x) &:= \frac{1}{2}\bar{\sigma}_f^2(x)(\omega+2\theta-1)(\omega+2\theta-2), \\ g_{01}(t,\omega,x) &:= -A_{01}(x)(\omega+\theta-1)(\omega+3\theta-2)(\omega+3\theta-3)\hat{P}_{\mathrm{CEV}}(t,\omega+3\theta-3,x), \\ g_{10}(t,\omega,x) &:= A_{10}(x)(\omega+\theta-1)\mathcal{D}^x_{1,1}\hat{P}_{\mathrm{CEV}}(t,\omega+\theta-1,x), \end{aligned} \tag{2.16}$$

respectively. The problems in (2.15) can be solved as

$$\begin{aligned} \hat{P}_{\mathrm{CEV}}(t,\omega,x) &= e^{\lambda(\omega,x)(T-t)}\,\hat{h}(\omega), \\ \hat{P}_{01}(t,\omega,x) &= -\int_t^T e^{\lambda(\omega,x)(\tilde{t}-t)}\,g_{01}(\tilde{t},\omega,x)\,d\tilde{t}, \\ \hat{P}_{10}(t,\omega,x) &= -\int_t^T e^{\lambda(\omega,x)(\tilde{t}-t)}\,g_{10}(\tilde{t},\omega,x)\,d\tilde{t}. \end{aligned} \tag{2.17}$$

Substituting (2.16) into (2.17), we obtain a closed-form expression of the approximate derivative price $\ddot{P}^{\epsilon,\delta} := P_{\mathrm{CEV}} + \sqrt{\epsilon}P_{01} + \sqrt{\delta}P_{10}$ explicitly as

$$\begin{aligned} \hat{\ddot{P}}^{\epsilon,\delta}(t,\omega,x) &= e^{\lambda(\omega,x)(T-t)}\,\hat{h}(\omega) \\ &\quad + \sqrt{\epsilon}\,A_{01}(x)(\omega+\theta-1)(\omega+3\theta-2)(\omega+3\theta-3)\,\frac{e^{\lambda(\omega,x)(T-t)}-e^{\lambda(\omega+3\theta-3,x)(T-t)}}{\lambda(\omega,x)-\lambda(\omega+3\theta-3,x)}\,\hat{h}(\omega+3\theta-3) \\ &\quad - \sqrt{\delta}\,A_{10}(x)(\omega+\theta-1)x\,\partial_x\lambda(\omega+\theta-1,x)\left(\frac{e^{\lambda(\omega,x)(T-t)}-e^{\lambda(\omega+\theta-1,x)(T-t)}}{(\lambda(\omega,x)-\lambda(\omega+\theta-1,x))^2}\right. \\ &\quad \left.-(T-t)\frac{e^{\lambda(\omega+\theta-1,x)(T-t)}}{\lambda(\omega,x)-\lambda(\omega+\theta-1,x)}\right)\hat{h}(\omega+\theta-1) \end{aligned} \tag{2.18}$$

in the domain of the Mellin transform.

The pricing formula (2.18) is given by a linear combination of terms that are in the form of a function of ω times the (shifted) Mellin transform of the payoff function h. Using the functions $\hat{h}_1(\omega)$, $\hat{h}_3(\omega)$, $\hat{A}^\epsilon(t,\omega,x)$ and $\hat{A}^\delta(t,\omega,x)$ defined by

$$\begin{aligned}
\hat{h}_1(\omega) &:= \hat{h}(\omega+(\theta-1)),\\
\hat{h}_3(\omega) &:= \hat{h}(\omega+3(\theta-1)),\\
\hat{A}_{\mathrm{CEV}}(t,\omega,x) &:= e^{\lambda(\omega,x)(T-t)},\\
\hat{A}^\epsilon(t,\omega,x) &:= \sqrt{\epsilon}\,A_{01}(x)(\omega+\theta-1)(\omega+3\theta-2)(\omega+3\theta-3)\,\frac{e^{\lambda(\omega,x)(T-t)}-e^{\lambda(\omega+3\theta-3,x)(T-t)}}{\lambda(\omega,x)-\lambda(\omega+3\theta-3,x)},\\
\hat{A}^\delta(t,\omega,x) &:= \sqrt{\delta}\,A_{10}(x)(\omega+\theta-1)x\partial_x\lambda(\omega+\theta-1,x)\left(\frac{e^{\lambda(\omega,x)(T-t)}-e^{\lambda(\omega+\theta-1,x)(T-t)}}{(\lambda(\omega,x)-\lambda(\omega+\theta-1,x))^2}\right.\\
&\qquad\left.-(T-t)\frac{e^{\lambda(\omega+\theta-1,x)(T-t)}}{\lambda(\omega,x)-\lambda(\omega+\theta-1,x)}\right)
\end{aligned} \tag{2.19}$$

and taking the inverse Mellin transform of $\hat{\ddot{P}}^{\epsilon,\delta}(t,\omega,x)$ in (2.18), $\ddot{P}^{\epsilon,\delta}(t,s,x)$ becomes

$$\begin{aligned}
\ddot{P}^{\epsilon,\delta}(t,s,x) &= \frac{1}{2\pi i}\int_{a-i\infty}^{a+i\infty}\hat{\ddot{P}}^{\epsilon,\delta}(t,\omega,x)\,s^{-\omega}\,d\omega\\
&= \frac{1}{2\pi i}\int_{a-i\infty}^{a+i\infty}\left[\hat{A}_{\mathrm{CEV}}(t,\omega,x)\,\hat{h}(\omega)+\hat{A}^\epsilon(t,\omega,x)\hat{h}_3(\omega)+\hat{A}^\delta(t,\omega,x)\hat{h}_1(\omega)\right]s^{-\omega}\,d\omega.
\end{aligned} \tag{2.20}$$

Note that the derivative price formula (2.20) requires computation of a single integral not like the case of the double integral in (2.14).

By the convolution theorem of the Mellin transform (cf. Srivastava and Buschman [25]) we rewrite the result (2.20) as the following simple expression in terms of Mellin convolution. The derivative price is expressed as a single integral representation.

Proposition 2.1. *Under the dynamics (2.1) of the underlying asset price, the derivative price defined by (2.3) is approximated by*

$$\ddot{P}^{\epsilon,\delta}(t,s,x) = \left(A_{\mathrm{CEV}} * h + A^\epsilon * h_3 + A^\delta * h_1\right)(t,s,x), \tag{2.21}$$

where h_1, h_3, A_{CEV}, A^ϵ and A^δ are the inverse Mellin transforms of $\hat{h}_1$, $\hat{h}_3$, $\hat{A}_{\mathrm{CEV}}$, $\hat{A}^\epsilon$ and $\hat{A}^\delta$ defined in (2.19), respectively and $*$ denotes the Mellin convolution.

From the properties of the Mellin transform (cf. Bracewell [26]), $\hat{h}_1(\omega)$ and $\hat{h}_3(\omega)$ defined in (2.19) lead to

$$\begin{aligned}
h_1(s) &= s^{\theta-1}h(s),\\
h_3(s) &= s^{3(\theta-1)}h(s),
\end{aligned}$$

respectively. The pricing formula (2.21) is expressed as the CEV price added by two correction terms related to A^ϵ (SVCEV volatility) and A^δ (SABR volatility). When ϵ and δ go to 0, the two terms A^ϵ and A^δ vanish and thus $\ddot{P}^{\epsilon,\delta}(t,s,x)$ becomes the CEV price, say $P_{\mathrm{CEV}}(t,s,x)$, which is given by $P_{\mathrm{CEV}}(t,s,x) = \left(A_{\mathrm{CEV}} * h\right)(t,s,x)$. So, the price formula (2.21) can be expressed as

$$\ddot{P}^{\epsilon,\delta}(t,s,x) = P_{\mathrm{CEV}}(t,s,x) + \left(A^\epsilon * h_3 + A^\delta * h_1\right)(t,s,x). \tag{2.22}$$

If we apply the following result obtained by Yoon and Kim [27] for the inverse Mellin transform

$$\mathcal{M}^{-1}\left(e^{a(\omega+b)^2}\right)(x) = \frac{1}{\sqrt{4a\pi}}x^b e^{-\frac{1}{4a}(\log x)^2},$$

to $\hat{A}_{\mathrm{CEV}}(t,\omega,x)$, then we obtain the following CEV price formula:

$$\begin{aligned}
P_{\mathrm{CEV}}(t,s,x) &= \int_0^\infty A_{\mathrm{CEV}}\left(t,\frac{s}{u},x\right)h(u)\frac{du}{u}\\
&= e^{-\frac{1}{8}\bar{\sigma}_f^2(x)(T-t)}\frac{1}{\sqrt{2\bar{\sigma}_f^2(x)(T-t)\pi}}\int_0^\infty\left(\frac{s}{u}\right)^{2\theta-\frac{3}{2}}e^{-\frac{1}{2\bar{\sigma}_f^2(x)(T-t)}\left(\log\left(\frac{s}{u}\right)\right)^2}h(u)\frac{du}{u}.
\end{aligned} \tag{2.23}$$

2.3. Near zero elasticity of variance

In this section, we consider the case that the elasticity of variance parameter θ is close to 1, that is, the elasticity of variance is close to 0 as formally defined as $2(\theta-1)$, based on the observation given by Kim et al. [28] for historical data on S&P 500 index. So, we define a parameter γ as

$$\gamma = 1-\theta$$

and assume that $0<\gamma\ll 1$.

We are interested in the approximation $\ddot{P}^{\epsilon,\delta,\gamma} := P_{000}+\sqrt{\epsilon}P_{010}+\sqrt{\delta}P_{100}+\gamma P_{001}$ of the expansion

$$P^{\epsilon,\delta,\gamma}(t,s,x,y)=\sum_{i,j,k=0}^{\infty}(\sqrt{\delta})^i(\sqrt{\epsilon})^j\gamma^k P_{ijk}(t,s,x,y). \tag{2.24}$$

Taking a Taylor expansion of $\hat{\hat{P}}^{\epsilon,\delta}(t,\omega,x)$ in (2.18) with respect to γ, we can obtain a formula for $\hat{\hat{P}}^{\epsilon,\delta,\gamma}(t,\omega,x)$. To present it concisely, we first observe that

$$\begin{aligned}
\lim_{\gamma\to 0}\frac{e^{\lambda(\omega,x)(T-t)}-e^{\lambda(\omega+3\theta-3,x)(T-t)}}{\lambda(\omega,x)-\lambda(\omega+3\theta-3,x)} &= (T-t)e^{\frac{1}{2}\bar{\sigma}_f^2(x)\omega(\omega+1)(T-t)},\\
\lim_{\gamma\to 0}\left[\frac{e^{\lambda(\omega,x)(T-t)}-e^{\lambda(\omega+\theta-1,x)(T-t)}}{(\lambda(\omega,x)-\lambda(\omega+\theta-1,x))^2}-(T-t)\frac{e^{\lambda(\omega+\theta-1,x)(T-t)}}{\lambda(\omega,x)-\lambda(\omega+\theta-1,x)}\right] &= \frac{1}{2}(T-t)^2e^{\frac{1}{2}\bar{\sigma}_f^2(x)\omega(\omega+1)(T-t)},\\
\lim_{\gamma\to 0}e^{\lambda(\omega,x)(T-t)} &= e^{\frac{1}{2}\bar{\sigma}_f^2(x)\omega(\omega+1)(T-t)},\\
\lim_{\gamma\to 0}\hat{h}_3(\omega)=\lim_{\gamma\to 0}\hat{h}_1(\omega) &= \hat{h}(\omega),
\end{aligned} \tag{2.25}$$

then we have

$$\hat{\hat{P}}^{\epsilon,\delta,\gamma}(t,\omega,x)=\hat{P}_{\mathrm{BS}}(t,\omega,x)\left[1+(T-t)\hat{A}_*^{\epsilon}(\omega,x)-(T-t)^2\hat{A}_*^{\delta}(\omega,x)-(T-t)\hat{A}_*^{\gamma}(\omega,x)\right], \tag{2.26}$$

where $\hat{P}_{\mathrm{BS}}$, $\hat{A}_*^{\epsilon}$, $\hat{A}_*^{\delta}$ and $\hat{A}_*^{\gamma}$ are

$$\begin{aligned}
\hat{P}_{\mathrm{BS}}(t,\omega,x) &:= e^{\frac{1}{2}\bar{\sigma}_f^2(x)\omega(\omega+1)(T-t)}\hat{h}(\omega),\\
\hat{A}_*^{\epsilon}(\omega,x) &:= \sqrt{\epsilon}\,A_{01}(x)\omega^2(\omega+1),\\
\hat{A}_*^{\delta}(\omega,x) &:= \frac{1}{2}\sqrt{\delta}\,A_{10}(x)x\bar{\sigma}_f(x)\bar{\sigma}_f'(x)\omega^2(\omega+1),\\
\hat{A}_*^{\gamma}(\omega,x) &:= \gamma\bar{\sigma}_f^2(x)(2\omega+1),
\end{aligned} \tag{2.27}$$

respectively.

As in the notation, $\hat{P}_{\mathrm{BS}}(t,\omega,x)$ is the Mellin transform of the Black-Scholes derivative price $P_{\mathrm{BS}}(t,s,x)$ with payoff h since the CEV price $\hat{P}_{\mathrm{CEV}}(t,\omega,x)$ is reduced to the Black-Scholes price when $\gamma\to 0$. Also, from the direct calculation of Panini and Srivastav [29], $\hat{P}_{\mathrm{BS}}(t,\omega,x)$ in (2.27) is exactly the same as the Mellin transform of the Black-Scholes price.

In order to calculate the inverse Mellin transform of $\hat{\hat{P}}^{\epsilon,\delta,\gamma}(t,\omega,x)$ given in (2.26), it is required to calculate the inverse Mellin transforms of $\omega\hat{P}_{\mathrm{BS}}$, $\omega^2\hat{P}_{\mathrm{BS}}$ and $\omega^3\hat{P}_{\mathrm{BS}}$. They can be obtained by using a property of Mellin transform given by

$$\mathcal{M}((\mathcal{D}_{1,1})^nP_{\mathrm{BS}})(\omega)=(-\omega)^n\hat{P}_{\mathrm{BS}}(t,\omega,x). \tag{2.28}$$

Then we obtain the following corollary of Proposition 2.1 for $\ddot{P}^{\epsilon,\delta,\gamma}(t,s,x)$.

Corollary 2.1. *Under the dynamics (2.1) of the underlying asset price where $0<\gamma\ll 1$ for $\theta := 1-\gamma$, the derivative price defined by (2.3) is approximated by*

$$\begin{aligned}
\ddot{P}^{\epsilon,\delta,\gamma}(t,s,x)=\big[P_{\mathrm{BS}} &+(T-t)a^{\epsilon}(x)\left(-(\mathcal{D}_{1,1})^3+(\mathcal{D}_{1,1})^2\right)P_{\mathrm{BS}}\\
&-(T-t)^2a^{\delta}(x)\left(-(\mathcal{D}_{1,1})^3+(\mathcal{D}_{1,1})^2\right)P_{\mathrm{BS}}\\
&-(T-t)a^{\gamma}(x)\left(-2\mathcal{D}_{1,1}+1\right)P_{\mathrm{BS}}\big](t,s,x),
\end{aligned} \tag{2.29}$$

where $a^{\epsilon}(x)$, $a^{\delta}(x)$ and $a^{\gamma}(x)$ are

$$\begin{aligned}
a^{\epsilon}(x) &:= \sqrt{\epsilon}A_{01}(x),\\
a^{\delta}(x) &:= \frac{1}{2}\sqrt{\delta}A_{10}(x)x\bar{\sigma}_f(x)\bar{\sigma}_f'(x),\\
a^{\gamma}(x) &:= \gamma\bar{\sigma}_f^2(x),
\end{aligned} \tag{2.30}$$

respectively.

According to Corollary 2.1, the derivative price $\ddot{P}^{\epsilon,\delta,\gamma}(t,s,x)$ can be calculated simply by taking a combination of the first, second and third derivatives (Delta, Gamma, and Speed, respectively) of the Black-Scholes price $P_{\mathrm{BS}}(t,s,x)$ with respect to the underlying price, which is a practically useful result. Here, $P_{\mathrm{BS}}(t,s,x)$ is the usual Black-Scholes price with volatility $\bar{\sigma}_f(x)$. The number of free parameters in the original SABR model is 4 while it is 9 in the case of the unified model. However, when it comes to the purpose of pricing derivatives, all the model parameters in the unified model are not required. In fact, they are absorbed into the four group parameters $\bar{\sigma}_f(x)$, $a^{\epsilon}_f(x)$, $a^{\delta}_s(x)$, and $a^{\gamma}(x)$ that are required to price the derivatives, as shown in Corollary 3.1. So, the methodology (asymptotic analysis) used here allows the unified model to be practically useful for the purpose of pricing derivatives.

The Black-Scholes price $P_{\mathrm{BS}}(t,s,x)$ is the limit of $\ddot{P}^{\epsilon,\delta,\gamma}(t,s,x)$ when all ϵ, δ and γ go to zero. If both ϵ and δ go to zero, then $\ddot{P}^{\epsilon,\delta,\gamma}(t,s,x)$ becomes the price of the CEV derivative P_{CEV}. In this way, we can find the pricing formulas of derivatives in the reduced models listed in Table 1. They are presented as follows:

$$\begin{aligned}
P_{\mathrm{CEV}} &= P_{\mathrm{BS}} - (T-t)a^{\gamma}(x)\left(-2D_{1,1}+1\right)P_{\mathrm{BS}},\\
P_{\mathrm{SV}_f} &= P_{\mathrm{BS}} + (T-t)a^{\epsilon}(x)\left(-D^3_{1,1}+D^2_{1,1}\right)P_{\mathrm{BS}},\\
P_{\mathrm{MSV}} &= P_{\mathrm{BS}} + (T-t)a^{\epsilon}(x)\left(-D^3_{1,1}+D^2_{1,1}\right)P_{\mathrm{BS}} - (T-t)^2a^{\delta}(x)\left(-D^3_{1,1}+D^2_{1,1}\right)P_{\mathrm{BS}},\\
P_{\mathrm{SVCEV}} &= P_{\mathrm{BS}} + (T-t)a^{\epsilon}(x)\left(-D^3_{1,1}+D^2_{1,1}\right)P_{\mathrm{BS}} - (T-t)a^{\gamma}(x)\left(-2D_{1,1}+1\right)P_{\mathrm{BS}},\\
P_{\mathrm{SABR}} &= P_{\mathrm{BS}} - (T-t)^2a^{\delta}(x)\left(-D^3_{1,1}+D^2_{1,1}\right)P_{\mathrm{BS}} - (T-t)a^{\gamma}(x)\left(-2D_{1,1}+1\right)P_{\mathrm{BS}},
\end{aligned} \tag{2.31}$$

where $D^3_{1,1} := (D_{1,1})^3$ and $D^2_{1,1} := (D_{1,1})^2$. All pricing formulas in (2.31) are expressed as the Black-Scholes derivative price plus additional terms related to the elasticity of variance, mean-reverting stochastic volatility, or SABR type of stochastic volatility. As observed in (2.1), there is a difference between the SABR-SVCEV model and the plain SABR model in terms of a function of the fast mean reversing process Y_t. This function becomes a constant as ϵ goes to zero. So, if this constant is chosen to be zero in the model, then the reference prices exactly become the price given by Hagan's formula in [1] when ϵ goes to zero.

3. Specific application

Once the pay-off function h is given for a considered derivative contract, the CEV price $P_{\mathrm{CEV}}(t,s,x)$ and the two convolutions constitute the fair price $\ddot{P}^{\epsilon,\delta}(t,s,x)$ of the derivative as shown in the formula (2.22). In the case where the elasticity of variance is close to zero, the formula (2.29) in Corollary 2.1. In this section, we apply this formula to two derivative contract cases, that is, the European vanilla option and the variance swap, and we obtain the price formulas concretely.

3.1. European vanilla option

In the case of a European put option with the payoff $h(s) = (K-s)^+$, we have $\hat{h}(\omega) = \frac{K^{\omega+1}}{\omega(\omega+1)}$ so that, from (2.19), $\hat{h}_1(\omega)$ and $\hat{h}_3(\omega)$ become

$$\begin{aligned}
\hat{h}_1(\omega) &= \frac{K^{\omega+\theta}}{(\omega+\theta-1)(\omega+\theta)},\\
\hat{h}_3(\omega) &= \frac{K^{\omega+3\theta-2}}{(\omega+3\theta-3)(\omega+3\theta-2)},
\end{aligned}$$

respectively. Then, by direct calculation, the put option price $\ddot{P}^{\epsilon,\delta}(t,s,x)$ is given by

$$\begin{aligned}
\ddot{P}^{\epsilon,\delta}(t,s,x) = {} & e^{-\frac{1}{8}\bar{\sigma}_f^2(x)(T-t)}\frac{1}{\sqrt{2\bar{\sigma}_f^2(x)(T-t)\pi}}\int_0^K \left(\frac{s}{u}\right)^{2\theta-\frac{3}{2}} e^{-\frac{1}{2\bar{\sigma}_f^2(x)(T-t)}\left(\log\left(\frac{s}{u}\right)\right)^2}(K-u)\frac{du}{u}\\
& + \frac{1}{2\pi i}\sqrt{\delta}A_{10}(x)\bar{\sigma}_f(x)\bar{\sigma}_f'(x)K^{\theta}\int_{a-i\infty}^{a+i\infty}\frac{(\omega+3\theta-2)(\omega+3\theta-3)}{\omega+\theta}\cdot\\
& \cdot\left(\frac{e^{\lambda(\omega,x)(T-t)}-e^{\lambda(\omega+\theta-1,x)(T-t)}}{(\lambda(\omega,x)-\lambda(\omega+\theta-1,x))^2} - (T-t)\frac{e^{\lambda(\omega+\theta-1,x)(T-t)}}{\lambda(\omega,x)-\lambda(\omega+\theta-1,x)}\right)\left(\frac{K}{s}\right)^{\omega}d\omega\\
& + \frac{1}{2\pi i}\sqrt{\epsilon}A_{01}(x)K^{3\theta-2}\int_{a-i\infty}^{a+i\infty}(\omega+\theta-1)\frac{e^{\lambda(\omega,x)(T-t)}-e^{\lambda(\omega+3\theta-3,x)(T-t)}}{\lambda(\omega,x)-\lambda(\omega+3\theta-3,x)}\left(\frac{K}{s}\right)^{\omega}d\omega,
\end{aligned} \tag{3.1}$$

where A_{10} and A_{01} are given by (2.10) and $\lambda(\omega,x)$ is given by (2.16).

When the elasticity of variance is close to 0, the well-known the Black-Scholes option price $P_{\mathrm{BS}}(t,s,x)$ given by Black, Scholes and Merton [11] or [30] applied to Corollary 2.1 leads to the put option price $\ddot{P}^{\epsilon,\delta,\gamma}(t,s,x)$. In fact, since we already have the CEV derivative price formula (2.23), specifying $\theta=1$ and $h(u)=(K-u)^+$ in (2.23) gives the following Black-Scholes put option price:

$$\begin{aligned} P_{\mathrm{BS}}(t,s,x) &= e^{-\frac{1}{8}\bar{\sigma}_f^2(x)(T-t)}\frac{1}{\sqrt{2\bar{\sigma}_f^2(x)(T-t)\pi}}\int_0^\infty \left(\frac{s}{u}\right)^{\frac{1}{2}} e^{-\frac{1}{2\bar{\sigma}_f^2(x)(T-t)}\left(\log\left(\frac{s}{u}\right)\right)^2}(K-u)^+\frac{du}{u} \\ &= e^{-\frac{1}{8}\bar{\sigma}_f^2(x)(T-t)}\frac{1}{\sqrt{2\bar{\sigma}_f^2(x)(T-t)\pi}}\int_{\log(s/K)}^\infty \left(Ke^{\frac{1}{2}v}-se^{-\frac{1}{2}v}\right)\exp\left(-\frac{v^2}{2\bar{\sigma}_f^2(T-t)}\right)dv \\ &= K\mathcal{N}(-d_2)-s\mathcal{N}(-d_1), \end{aligned} \tag{3.2}$$

where $\mathcal{N}$ denotes the standard normal cumulative distribution function and d_1 and d_2 are

$$d_1 := \frac{1}{\bar{\sigma}_f(x)\sqrt{T-t}}\left(\log(s/K)+\frac{1}{2}\bar{\sigma}_f^2(x)(T-t)\right),\quad d_2 := d_1-\bar{\sigma}_f(x)\sqrt{T-t},$$

respectively. Plugging the Black-Scholes price (3.2) into (2.29) in Corollary 2.1, we obtain the following put option price formula:

$$\begin{aligned} \ddot{P}^{\epsilon,\delta,\gamma}_{\mathrm{put}}(t,s,x) &= K\mathcal{N}(-d_2)-s\mathcal{N}(-d_1) \\ &\quad+\frac{a^\epsilon(x)-a^\delta(x)}{\sigma^3}\left(K\mathcal{N}'''(-d_2)-s\mathcal{N}'''(-d_1)\right)\frac{1}{\sqrt{T-t}} \\ &\quad+\frac{a^\epsilon(x)-a^\delta(x)}{\sigma^2}\left(K\mathcal{N}''(-d_2)+2s\mathcal{N}''(-d_1)\right) \\ &\quad-\left[\frac{a^\epsilon(x)-a^\delta(x)}{\sigma}s\mathcal{N}'(-d_1)+2\frac{a^\gamma(x)}{\sigma}\left(K\mathcal{N}'(-d_2)-s\mathcal{N}'(-d_1)\right)\right]\sqrt{T-t} \\ &\quad-a^\gamma(x)\left(K\mathcal{N}(-d_2)+s\mathcal{N}(-d_1)\right)(T-t), \end{aligned} \tag{3.3}$$

where $a^\epsilon(x)$, $a^\delta(x)$ and $a^\gamma(x)$ are given by (2.30). We note that the range of the order of terms in the above formula is from $\frac{1}{\sqrt{T-t}}$ to $T-t$, which suggests the ability of the model structure to capture the market's diverse maturity-dependent view of the likelihood of future changes in a given security's price.

Now, we check the price gap between the unified SABR-SVCEV model and the four reduced models (CEV, SVCEV, SV_f and MSV) using the price formulas given in (2.29) and (2.31) in the case of a European call option. As shown in Fig. 1, the price gap reverses its sign when the option is near the money and exhibits non-linearity with respect to the price of the underlying asset in the case of the CEV and SVCEV models. However, the price gap between the unified model and the SV_f and MSV models exhibits an almost linear relationship and continues to grow in the same direction within a range of the prices of the underlying assets. This observed difference between the two types of volatility models is attributed to the inclusion or absence of the parameter θ that captures the elasticity of variance.

3.2. Variance swap

A variance swap is one of the volatility derivatives as a forward contract with a pay-off given by the realized variance of the underlying asset. The contract is settled based on the difference between the realized variance and the predetermined variance strike. The realized variance and volatility swap contracts are discretely sampled, but term sheets of these kinds of contracts are designated on a daily monitoring basis, and thus continuous sampling assumption may cause an ignorable approximation error. Refer to Broadie and Jain [31] and Jarrow et al. [32] for discussion of the continuously sampled approximation.

From the no-arbitrage argument and the Itô formula, the fair variance swap strike, $K^{\epsilon,\delta}_{\mathrm{var}}$, is given by

$$K^{\epsilon,\delta}_{\mathrm{var}}(t,s,x,y) = -\frac{2}{T-t}E^{\mathbb{Q}}[\log\left(\frac{S_T}{s}\right)\mid S_t=s,X_t=x,Y_t=y]. \tag{3.4}$$

So, to price the fair variance swap strike, we need to calculate

$$P^{\epsilon,\delta}_{\mathrm{var}}(t,s,x,y) = E^{\mathbb{Q}}[\log(S_T)\mid S_t=s,X_t=x,Y_t=y]. \tag{3.5}$$

This corresponds to choosing the payoff function h in (2.3) as the logarithmic function. By specifying the function $h(u)=\log u$ and $\theta=1$ in (2.23), we have the following Black-Scholes value of (3.5):

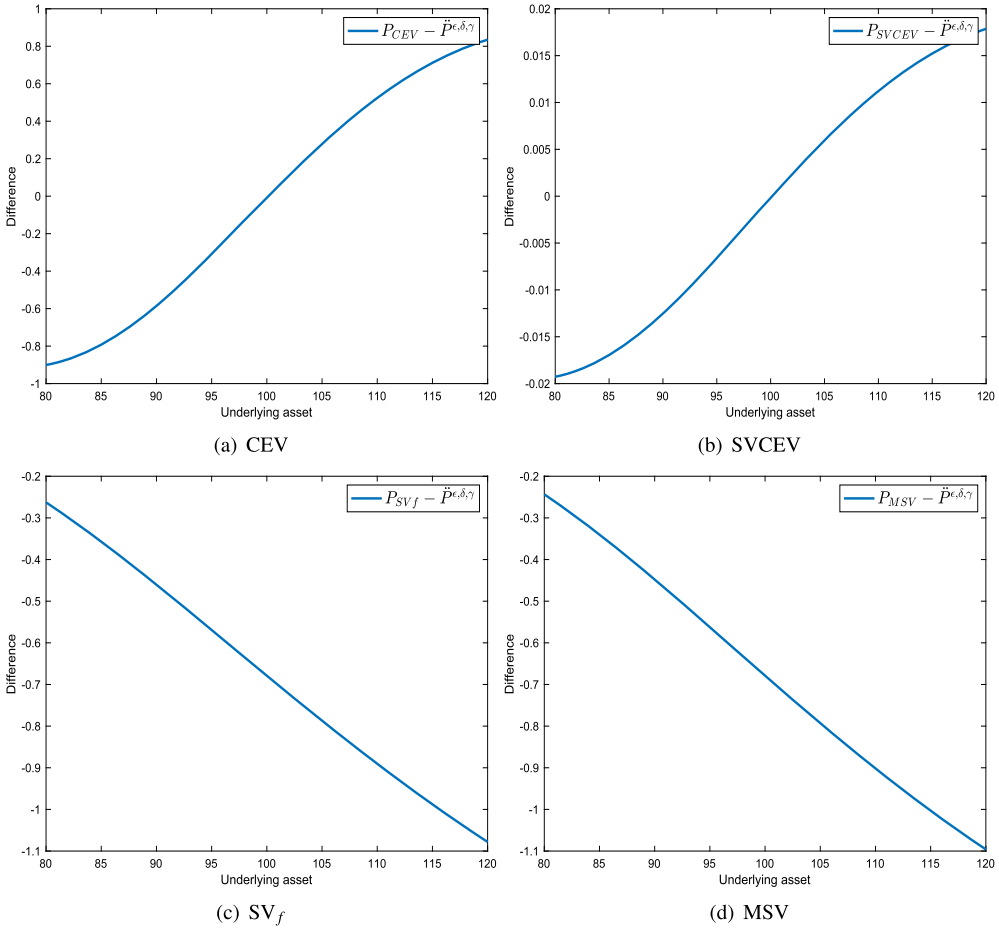

Fig. 1. Price gap between the SABR-SVCEV model and the four reduced models (CEV, SVCEV, SV$_f$ and MSV) for a European call; Maturity = 1.0, Strike price = 100, $x_0 = 0.1, r = 0.3, \rho_s y = -0.2, \rho_s x = 0.2, \rho_x y = 0.2, \epsilon = 0.1, \delta = 0.01, \gamma = 0.1$, $\alpha(Y_t) = m - Y_t, \beta(Y_t) = \sigma, m = \log(0.1), f(x) = \exp(x)$.

$$
\begin{aligned}
P_{\text{var}}^{\text{BS}}(t,s,x) &= e^{-\frac{1}{8}\bar{\sigma}_f^2(x)(T-t)} \frac{1}{\sqrt{2\bar{\sigma}_f^2(x)(T-t)\pi}} \int_0^\infty \left(\frac{s}{u}\right)^{\frac{1}{2}} e^{-\frac{1}{2\bar{\sigma}_f^2(x)(T-t)}\left(\log\left(\frac{s}{u}\right)\right)^2} \log u \, \frac{du}{u} \\
&= e^{-\frac{1}{8}\bar{\sigma}_f^2(x)(T-t)} \frac{1}{\sqrt{2\bar{\sigma}_f^2(x)(T-t)\pi}} \int_{-\infty}^\infty e^{-\frac{1}{2\bar{\sigma}_f^2(x)(T-t)}v^2 + \frac{1}{2}v} (\log s - v)\, dv \\
&= \log s - \frac{1}{2}\bar{\sigma}_f^2(x)(T-t).
\end{aligned} \tag{3.6}
$$

Substituting this Black-Scholes value into (2.29) in Corollary 2.1, we obtain the following first order approximation result:

$$
\ddot{P}_{\text{var}}^{\epsilon,\delta,\gamma}(t,s,x) = \log s - \frac{1}{2}\bar{\sigma}_f^2(x)(T-t) - a^\gamma(x)(T-t)\left(\log s - \frac{1}{2}\bar{\sigma}_f^2(x)(T-t) - 2\right), \tag{3.7}
$$

where $a^\gamma(x)$ is given by (2.30). Then, from (3.4), (3.5), and (3.7), the approximate fair variance swap strike value is

$$
\ddot{K}_{\text{var}}^{\epsilon,\delta,\gamma}(t,s,x) = \bar{\sigma}_f^2(x) + 2a^\gamma(x)\left(\log s - \frac{1}{2}\bar{\sigma}_f^2(x)(T-t) - 2\right). \tag{3.8}
$$

4. Numerical results

In this section, we first check the accuracy of the price formula (2.29) given in Corollary 2.1 using a Monte Carlo simulation. Second, we show the convergence of the SABR-SVCEV model to the reduced models listed in Table 1 under various market conditions when the corresponding parameters reach 0. Third, we compare the SABR-SVCEV model with the SABR model in terms of the implied volatility data fit of a foreign exchange option. Finally, the analytic expression for a variance swap is tested numerically.

Table 2
Error of implied volatility between the SABR-SVCEV model and MC simulation for $T = 0.021$ (a week), where average elapsed time is less than 0.01 seconds for all the number of simulations.

Panel A : ATM			Error (%)	
Parameters $(\epsilon, \delta, \gamma)$	Simul.	10000	50000	100000
$(0.150, 0.10, 0.10)$		82.2282	82.9710	81.7198
$(0.075, 0.05, 0.05)$		34.9586	34.8572	35.5677
$(0.015, 0.01, 0.01)$		3.4904	0.4586	0.1991
Panel B : ITM (Moneyness = 95%)			Error (%)	
Parameters $(\epsilon, \delta, \gamma)$	Simul.	10000	50000	100000
$(0.150, 0.10, 0.10)$		97.3077	98.0035	98.2905
$(0.075, 0.05, 0.05)$		43.9167	41.1274	42.6066
$(0.015, 0.01, 0.01)$		0.9917	2.2707	1.2090
Panel C : OTM (Moneyness = 105%)			Error (%)	
Parameters $(\epsilon, \delta, \gamma)$	Simul.	10000	50000	100000
$(0.150, 0.10, 0.10)$		14.0826	13.9444	14.0056
$(0.075, 0.05, 0.05)$		6.5980	7.3184	7.3110
$(0.015, 0.01, 0.01)$		0.8413	1.0581	1.1116

From Corollary 2.1, we note that all original model parameters are not required to price derivatives. In fact, the number of necessary parameters and functions for the derivative price is considerably reduced from 9 to 4 as follows.

$$\gamma,\ \delta,\ \epsilon,\ f(x,y),\ \alpha(y),\ \beta(y),\ \rho_{sx},\ \rho_{sy},\ \rho_{xy} \quad \Longrightarrow \quad \bar{\sigma}_f(x),\ a^{\epsilon}_f(x),\ a^{\delta}_s(x),\ a^{\gamma}(x)$$

In order to estimate the pricing parameters $\bar{\sigma}_f(x)$, $a^{\epsilon}_f(x)$, $a^{\delta}_s(x)$, and $a^{\gamma}(x)$ (or γ), we can utilize calibration from near-the-money European call option implied volatilities, where the implied volatility is defined as σ_{analytic} satisfying the equation $P_{\text{BS}}(t, s; \sigma_{\text{analytic}}) = \ddot{P}^{\epsilon,\delta,\gamma}(t, s, x)$, where P_{BS} stands for the classical Black-Scholes formula.

The calculations are performed across six option maturities (1 week, 1 month, 3 months, 6 months, 1 year, and 2 years) and three different levels of moneyness (at the money (ATM), in the money (ITM), and out of the money (OTM)). The parameters and functions commonly used in numerical work are given by $S = 100$, $X = 0.1$, $Y = -1.0$, $r = 0.03$, $\rho_{sx} = 0.1$, $\rho_{sy} = -0.1$, $\rho_{xy} = 0.1$, $m = \log(0.1)$, and $f(x) = \exp(x)$ and the process Y_t is assumed to follow an Ornstein-Uhlenbeck process defined by $\alpha(Y_t) = \log(0.1) - Y_t$ and $\beta(Y_t) = 0.1$.

4.1. Accuracy

We first present the differences (errors) between the pricing results of the Monte Carlo (MC) simulation and the analytic formula (2.29) in terms of implied volatility. Here, the error is defined as

$$\text{Error}\,(\%) = \left|\sigma_{\text{analytic}} - \sigma_{\text{MC}}\right| \times 100,$$

where σ_{analytic} is the implied volatility calculated by using the analytic formula (2.29) in Corollary 2.1 and σ_{MC} is the implied volatility generated by the MC simulation.

In Tables 2–7, we present MC simulation results (error and computational cost) for various time-to-maturity (T), namely, one week, one month, three months, six months, one year, and two years, across ATM, ITM and OTM cases. The results indicate that the implied volatility error tends to diminish as the parameter values approach zero, reflecting the improved accuracy of the SABR-SVCEV model under such conditions. This indicates that the derived formula provides reasonable accuracy in modeling the volatility term structure. However, it is important to note that, for longer time-to-maturities, convergence is only observable when the parameter values are sufficiently small. This is due to the influence of the time step size inherent in the MC simulation. Consequently, the parameter sets used in our simulations were adjusted to smaller scales for longer time-to-maturities. This adjustment leads to an increase in computational time as time-to-maturity lengthens. Although this may be a critical issue from a practical point of view, we emphasize that the primary contribution of this study lies in the derivation of an analytic pricing formula under the SABR-SVCEV model. Moreover, the computational burden associated with MC simulations can be significantly mitigated through high performance computing techniques, such as parallel computing discussed as, for example, in LeBeau [34] and Alerstam et al. [35].

4.2. Convergence to reduced models

We now examine whether the proposed unified model (the SABR-SVCEV model) converges to the individual models listed in Table 1 under various market conditions. Figs. 2 and 3 illustrate how the unified model converges to each reduced model at various types of time-to-maturity (1 month, 6 months, 1 year, and 2 years) and moneyness conditions (ATM, ITM, OTM). In terms of the absolute pricing error defined by

Table 3
Error of implied volatility between the SABR-SVCEV model and MC simulation for $T = 0.083$ (a month), where average elapsed time (in seconds) is 0.73, 2.44, and 5.25 for 10000, 50000, and 100000, respectively.

Panel A : ATM			Error (%)	
Parameters $(\epsilon, \delta, \gamma)$	Simul.	10000	50000	100000
$(0.0150, 0.010, 0.010)$		4.4079	3.8531	3.7285
$(0.0075, 0.005, 0.005)$		1.5990	2.9200	1.5219
$(0.0015, 0.001, 0.001)$		0.9275	0.3720	0.4233
Panel B : ITM (Moneyness = 90%)			Error (%)	
Parameters $(\epsilon, \delta, \gamma)$	Simul.	10000	50000	100000
$(0.0150, 0.010, 0.010)$		27.2932	15.4490	15.2040
$(0.0075, 0.005, 0.005)$		13.2296	8.7595	8.9836
$(0.0015, 0.001, 0.001)$		1.1299	0.2372	0.0840
Panel C : OTM (Moneyness = 110%)			Error (%)	
Parameters $(\epsilon, \delta, \gamma)$	Simul.	10000	50000	100000
$(0.0150, 0.010, 0.010)$		1.0574	1.0282	1.0347
$(0.0075, 0.005, 0.005)$		0.6399	0.5628	0.4267
$(0.0015, 0.001, 0.001)$		0.4446	0.3970	0.0663

Table 4
Error of implied volatility between the SABR-SVCEV model and MC simulation for $T = 0.25$ (three months), where average elapsed time (in seconds) is 0.71, 2.49, and 5.32 for 10000, 50000, and 100000, respectively.

Panel A : ATM			Error (%)	
Parameters $(\epsilon, \delta, \gamma)$	Simul.	10000	50000	100000
$(0.0150, 0.010, 0.010)$		11.1156	8.0231	7.6164
$(0.0075, 0.005, 0.005)$		5.5707	4.5135	3.8857
$(0.0015, 0.001, 0.001)$		1.9116	0.7806	0.5868
Panel B : ITM (Moneyness = 90%)			Error (%)	
Parameters $(\epsilon, \delta, \gamma)$	Simul.	10000	50000	100000
$(0.0150, 0.010, 0.010)$		25.1200	21.5128	20.1508
$(0.0075, 0.005, 0.005)$		13.4535	11.1906	10.6672
$(0.0015, 0.001, 0.001)$		1.5466	1.8281	0.8064
Panel C : OTM (Moneyness = 110%)			Error (%)	
Parameters $(\epsilon, \delta, \gamma)$	Simul.	10000	50000	100000
$(0.0150, 0.010, 0.010)$		4.8870	4.1641	3.7880
$(0.0075, 0.005, 0.005)$		2.4666	1.7603	1.7855
$(0.0015, 0.001, 0.001)$		0.4480	0.0836	0.0733

$$\text{Error} = \left| \ddot{P}^{\epsilon,\delta,\gamma} - P_{\text{reduced model}} \right|,$$

where $\ddot{P}^{\epsilon,\delta,\gamma}$ is the option price (2.29) in Corollary 2.1 and $P_{\text{reduced model}}$ is the option price corresponding to one of BS (Black-Scholes), CEV, SV_f, MSV, SVCEV, and SABR models, each subfigure of Figs. 2 and 3 shows that the error between the unified model and each reduced model approaches zero as the associated parameters tend toward zero, regardless of maturity and moneyness, as is naturally expected. Furthermore, Fig. 4 presents the convergence results under varying volatility environments. Although the shape of convergence differs depending on the level of volatility, the absolute error in option prices consistently converges to zero. These results collectively confirm that the unified model successfully reduces to the respective individual models across a wide range of market conditions.

4.3. Model calibration

To further assess the practical relevance of incorporating a mean-reverting volatility component into the SABR framework, we evaluated the calibration performance of the proposed unified model. Specifically, we compare its calibration accuracy against that of the standard SABR model using foreign exchange (FX) option data. FX option is chosen here because of its implied volatility structure, which exhibits a more pronounced U-shape compared to the implied volatilities observed in stock option markets. In order to calibrate the pricing parameters, we minimize the difference between the market-implied volatilities and the model-implied volatilities using

Table 5
Error of implied volatility between the SABR-SVCEV model and MC simulation for $T = 0.5$ (6 months), where average elapsed time (in seconds) is 1.05, 3.19, and 6.65 for 10000, 50000, and 100000, respectively.

Panel A : ATM			Error (%)	
Parameters $(\epsilon, \delta, \gamma)$	Simul.	10000	50000	100000
$(0.0150, 0.010, 0.010)$		13.5113	10.2794	10.3761
$(0.0075, 0.005, 0.005)$		6.9042	5.4265	5.4196
$(0.0015, 0.001, 0.001)$		1.9986	0.1249	0.1416
Panel B : ITM (Moneyness = 90%)			Error (%)	
Parameters $(\epsilon, \delta, \gamma)$	Simul.	10000	50000	100000
$(0.0150, 0.010, 0.010)$		53.6939	40.8137	39.2071
$(0.0075, 0.005, 0.005)$		24.9460	19.7365	20.4172
$(0.0015, 0.001, 0.001)$		2.7613	0.3048	0.3041
Panel C : OTM (Moneyness = 110%)			Error (%)	
Parameters $(\epsilon, \delta, \gamma)$	Simul.	10000	50000	100000
$(0.0150, 0.010, 0.010)$		43.2133	32.5328	31.7120
$(0.0075, 0.005, 0.005)$		16.7617	16.5213	16.4421
$(0.0015, 0.001, 0.001)$		1.1646	0.8123	0.1278

Table 6
Error of implied volatility between the SABR-SVCEV model and MC simulation for $T = 1.0$ (1 year), where average elapsed time (in seconds) is 223.62, 1422.78, and 2718.74 for 10000, 50000, and 100000, respectively.

Panel A : ATM			Error (%)	
Parameters $(\epsilon, \delta, \gamma)$	Simul.	10000	50000	100000
$(0.0750, 0.050, 0.050)$		16.0883	15.5353	15.0845
$(0.0015, 0.001, 0.001)$		6.3214	6.8028	7.1443
$(0.00015, 0.0001, 0.0001)$		0.5419	0.8858	0.3184
Panel B : ITM (Moneyness = 90%)			Error (%)	
Parameters $(\epsilon, \delta, \gamma)$	Simul.	10000	50000	100000
$(0.0750, 0.050, 0.050)$		20.2728	19.5273	19.1683
$(0.0015, 0.001, 0.001)$		10.4328	10.4978	8.7611
$(0.00015, 0.0001, 0.0001)$		0.6165	0.6114	0.1638
Panel C : OTM (Moneyness = 110%)			Error (%)	
Parameters $(\epsilon, \delta, \gamma)$	Simul.	10000	50000	100000
$(0.0750, 0.050, 0.050)$		5.8558	5.1455	5.1469
$(0.0015, 0.001, 0.001)$		3.3500	3.2220	3.1258
$(0.00015, 0.0001, 0.0001)$		0.3975	0.2169	0.5933

the GBP/USD option, 3 March 2020. Specifically, we collect data for six maturities (1 month, 2 months, 3 months, 6 months, 1 year, and 2 years) and consider 17 moneynesses spanning from 80% to 120% for each maturity. The minimization is expressed as

$$\underset{\bar{\sigma}_f, a_f^{\epsilon}, a_s^{\delta}, \gamma}{\operatorname{argmin}} \left[\sum_{T_i} \sum_{K_j} \left(\sigma_{K_j,\text{mkt}}^{T_i} - \sigma_{K_j,\text{model}}^{T_i} \right)^2 \right],$$

where $\sigma_{K_j,\text{mkt}}^{T_i}$ denotes the implied volatility of the FX option market, obtained from Reuters, and $\sigma_{K_j,\text{model}}^{T_i}$ represents the implied volatility generated by the SABR or unified model for an option with strike K_j and maturity T_i. Here, the Levenberg-Marquardt algorithm (cf. Marquardt [33]), one of the well-known numerical optimization techniques, was used to determine the optimal values of the pricing parameters. This calibration process ensures that the model's outputs align closely with observed market values. Based on the selected option price data, Fig. 5 presents the calibration results for SABR and SABR-SVCEV models in terms of implied volatility, where $\alpha(Y_t) = m - Y_t$, $\beta(Y_t) = \sigma$, $m = \log(0.1)$, and $f(x) = \exp(x)$ have been used. The implied volatilities generated by the SABR model and the unified model are compared with each other, and the volatilities implied by the market option prices. Also, the error between the market-implied volatility and the model-implied volatility is computed for the SABR and unified models, where the Error in Fig. 5 for each i-th maturity is defined as

Table 7
Error of implied volatility between the SABR-SVCEV model and MC simulation for $T = 2.0$ (2 year), where average elapsed time (in seconds) is 10.62, 4169.14, and 8979.15 for 10000, 50000, and 100000, respectively.

Panel A : ATM			Error (%)	
Parameters $(\epsilon, \delta, \gamma)$	Simul.	10000	50000	100000
$(0.0750, 0.050, 0.050)$		30.5278	28.9065	28.1902
$(0.0015, 0.001, 0.001)$		13.1217	12.9401	13.4808
$(0.00015, 0.0001, 0.0001)$		0.5384	0.6143	0.1494
Panel B : ITM (Moneyness = 90%)			**Error (%)**	
Parameters $(\epsilon, \delta, \gamma)$	Simul.	10000	50000	100000
$(0.0750, 0.050, 0.050)$		31.1716	29.7023	29.6859
$(0.0015, 0.001, 0.001)$		16.8858	14.7969	14.9227
$(0.00015, 0.0001, 0.0001)$		0.4330	0.9396	0.5744
Panel C : OTM (Moneyness = 110%)			**Error (%)**	
Parameters $(\epsilon, \delta, \gamma)$	Simul.	10000	50000	100000
$(0.0750, 0.050, 0.050)$		6.8547	6.4990	6.7413
$(0.0015, 0.001, 0.001)$		5.2517	5.0006	4.8404
$(0.00015, 0.0001, 0.0001)$		0.2374	0.1951	0.5246

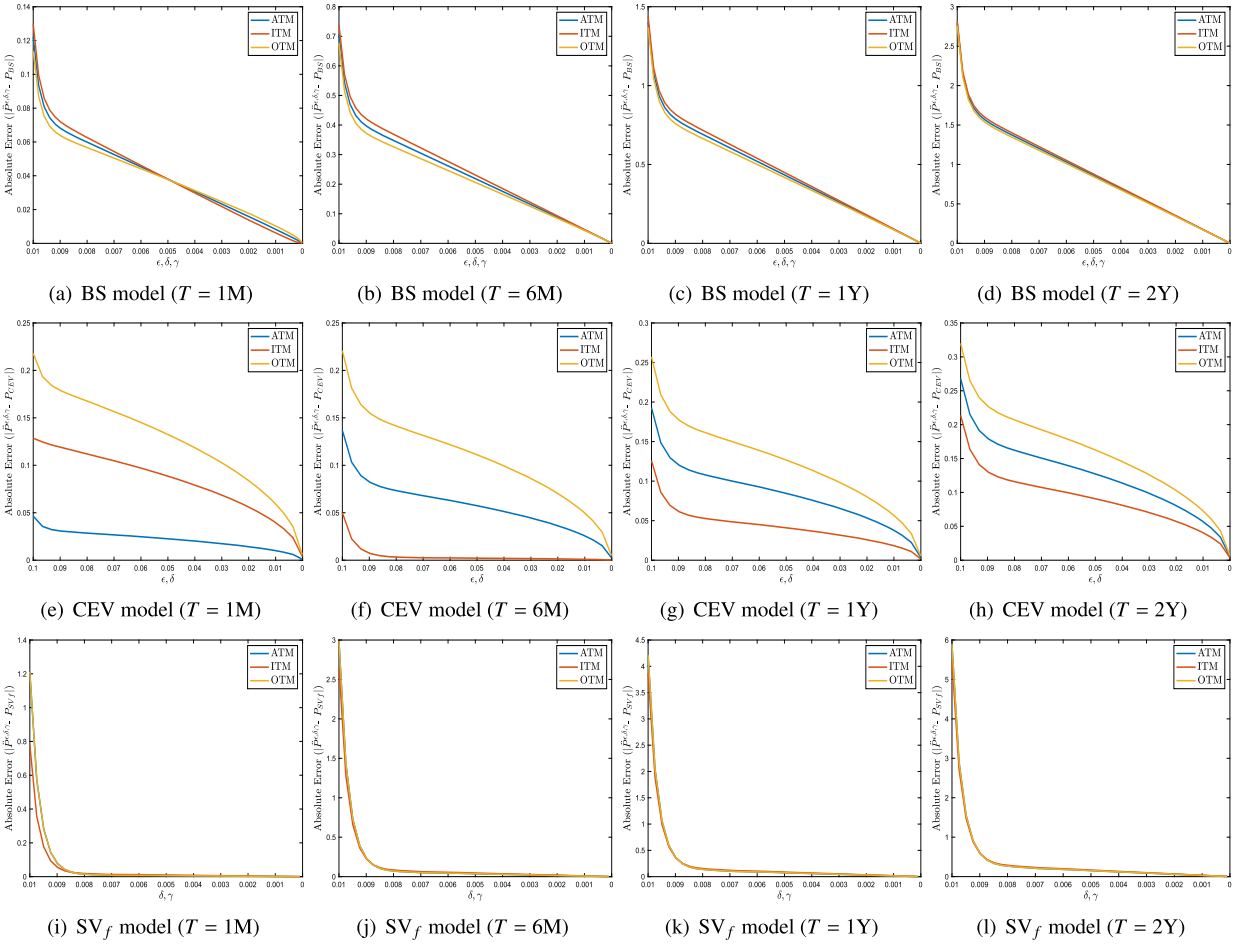

(a) BS model ($T = 1$M) (b) BS model ($T = 6$M) (c) BS model ($T = 1$Y) (d) BS model ($T = 2$Y)

(e) CEV model ($T = 1$M) (f) CEV model ($T = 6$M) (g) CEV model ($T = 1$Y) (h) CEV model ($T = 2$Y)

(i) SV_f model ($T = 1$M) (j) SV_f model ($T = 6$M) (k) SV_f model ($T = 1$Y) (l) SV_f model ($T = 2$Y)

Fig. 2. Convergence of option prices under the unified model to those under the reduced models (BS, CEV, and SV_f) for different time-to-maturity and moneyness.

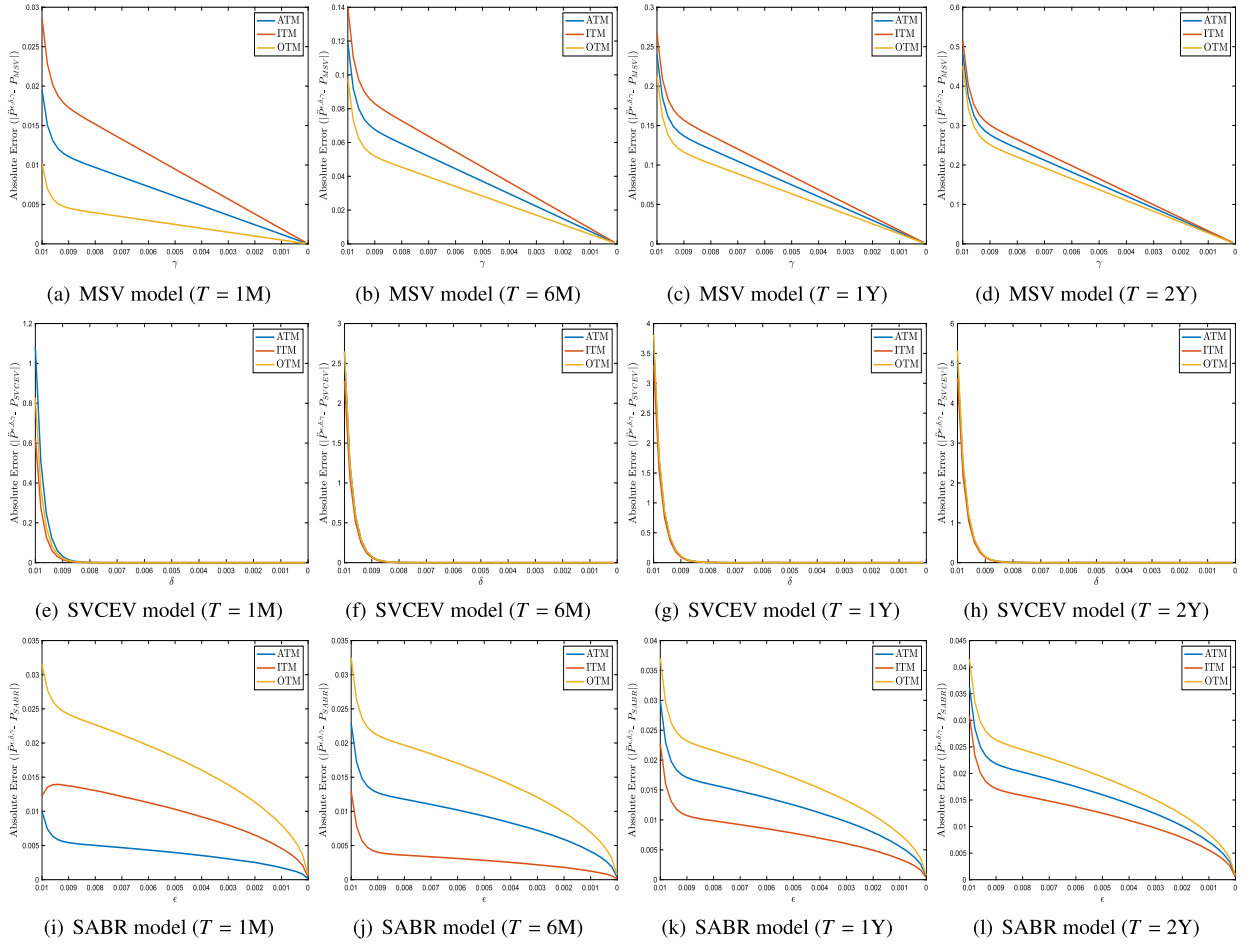

(a) MSV model (T = 1M) (b) MSV model (T = 6M) (c) MSV model (T = 1Y) (d) MSV model (T = 2Y)

(e) SVCEV model (T = 1M) (f) SVCEV model (T = 6M) (g) SVCEV model (T = 1Y) (h) SVCEV model (T = 2Y)

(i) SABR model (T = 1M) (j) SABR model (T = 6M) (k) SABR model (T = 1Y) (l) SABR model (T = 2Y)

Fig. 3. Convergence of option prices under the unified model to those under the reduced models (MSV, SVCEV, and SABR) for different time-to-maturity and moneyness.

$$\text{Error}_i = \frac{1}{17}\sum_{j=1}^{17}\left|\sigma^{T_i}_{K_j,\text{mkt}} - \sigma^{T_i}_{K_j,\text{model}}\right|,$$

where $\sigma^{T_i}_{K_j,\text{mkt}}$ and $\sigma^{T_i}_{K_j,\text{model}}$ represent the market- and model-implied volatilities with the j-th option strike, respectively. The following facts can be observed. First, the unified model demonstrates superior calibration performance compared to the SABR model. In particular, the unified model starts capturing the convexity of the implied volatility curves of the market for short time-to-maturities with the first-order price approximation. Second, it should be noted that the unified model tends to exhibit an increasing calibration error as the time-to-maturity becomes shorter. This should be attributed to the fact that we employ an approximation that represents only the first-order correction, thereby requiring higher-order correction terms for more accurate capture of the U-shaped structure.

4.4. Test on variance swap

In this section, we present some numerical results to support the findings related to variance swaps given in Section 3. Considering various values (0.1, 0.05, 0.01) of ϵ and (0.1, 0.05, 0.01) of γ in the context of the SABR-SVCEV model, we demonstrate the functional behavior of $\check{P}^{\epsilon,\delta,\gamma}_{\text{var}}$ (from now on we call it the P-function) and the fair strike $\check{K}^{\epsilon,\delta,\gamma}_{\text{var}}$ given by (3.7) and (3.8), respectively, with respect to the time-to-maturity, and compare the results with the well-known Black-Scholes case.

Fig. 6 shows the results. The key findings shown in this figure are as follows. First, there are significant differences in both the P-function and the fair strike between the SABR-SVCEV model and the Black-Scholes model, in particular, when the remaining maturity is long. Second, as the time-to-maturity approaches zero, the difference in the P-function between the two models converges to zero, while the difference in the fair strike converges to a non-zero level. This is due to the presence of the term $T-t$ in the denominator of (3.4). Furthermore, the results in the SABR-SVCEV model are closer to those of the Black-Scholes model, as the parameter γ becomes zero.

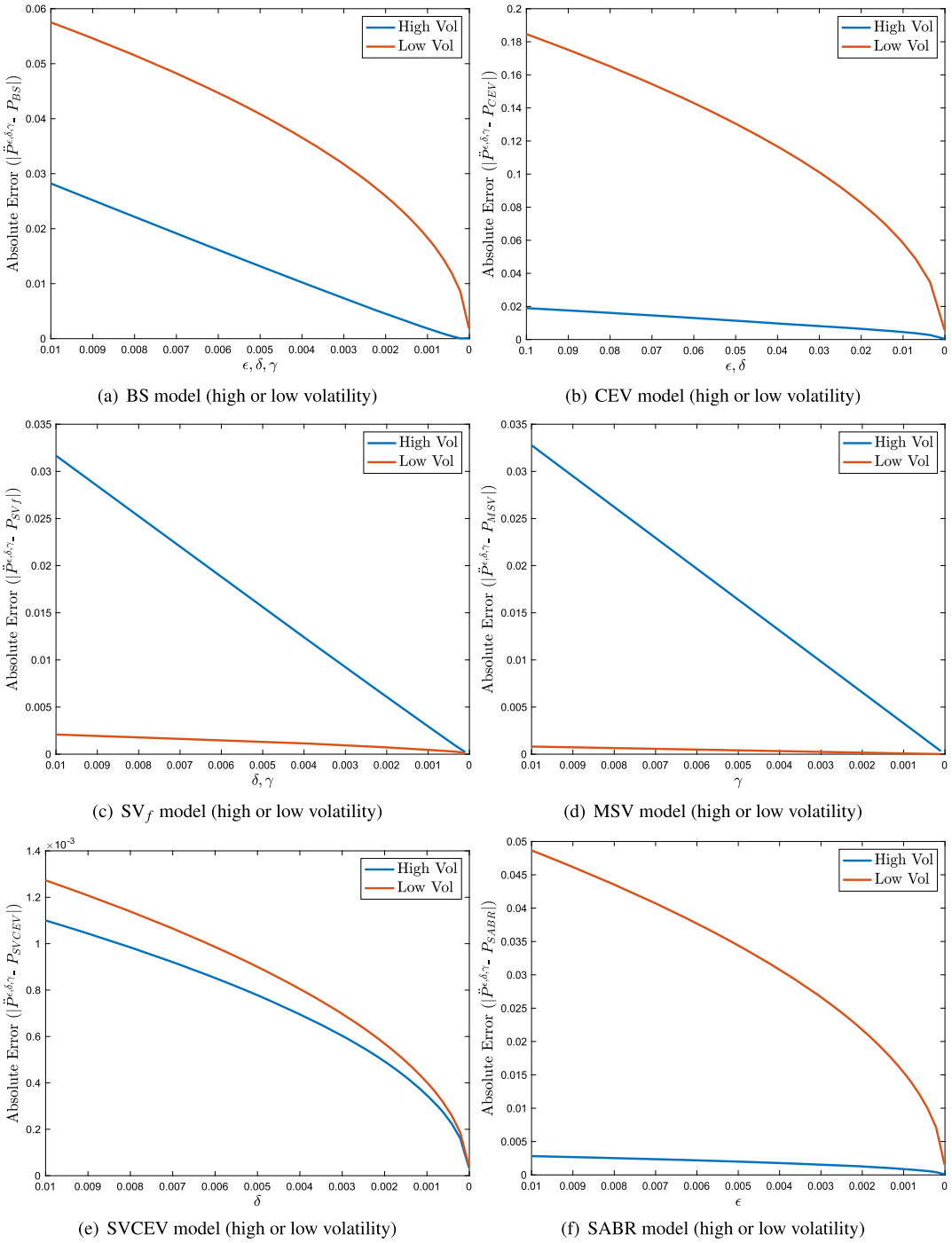

(a) BS model (high or low volatility)

(b) CEV model (high or low volatility)

(c) SV_f model (high or low volatility)

(d) MSV model (high or low volatility)

(e) SVCEV model (high or low volatility)

(f) SABR model (high or low volatility)

Fig. 4. Convergence of option prices under the unified model to those under the reduced models (BS, CEV, SV_f, MSV, SVCEV, and SABR) for different volatility regimes, where the time-to-maturity is one month, and the high and low volatility levels are set to be $\sigma = 1.0$ and $\sigma = 0.01$, respectively.

Notably, we observe that for smaller values of ϵ, the fair strike values in the SABR-SVCEV model exhibit sharper changes in the short time-to-maturity region (see Fig. 6-(b), (d), and (f)). This indicates that the SABR-SVCEV model allows for more flexible pricing results compared to the Black-Scholes model, in particular, for contracts with short remaining maturities.

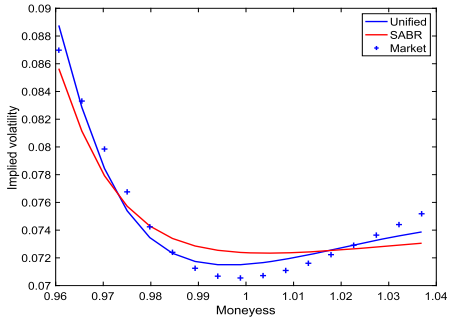

(a) Time to maturity = 1M

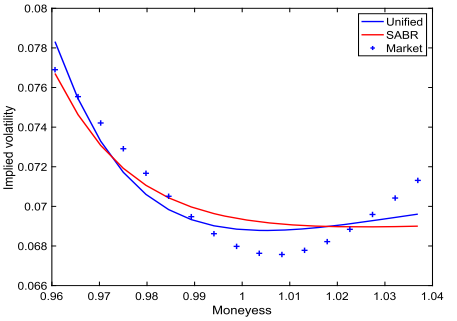

(b) Time to maturity = 2M

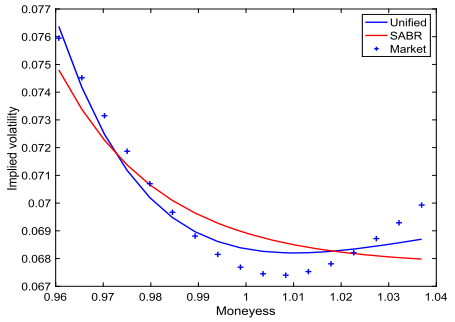

(c) Time to maturity = 3M

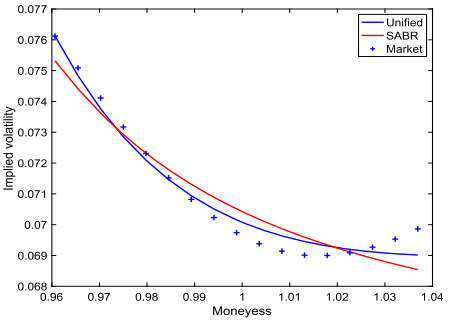

(d) Time to maturity = 6M

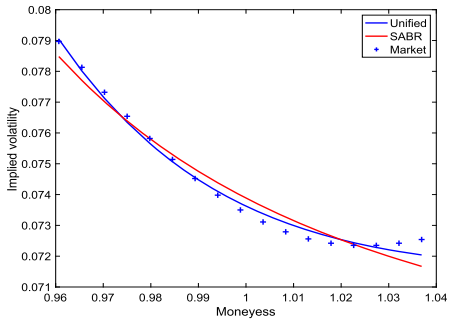

(e) Time to maturity = 9M

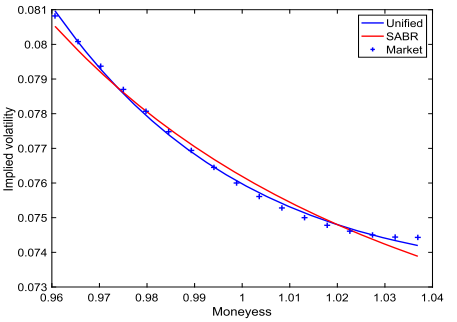

(f) Time to maturity = 1Y

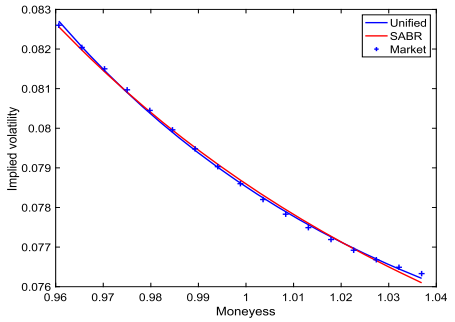

(g) Time to maturity = 2Y

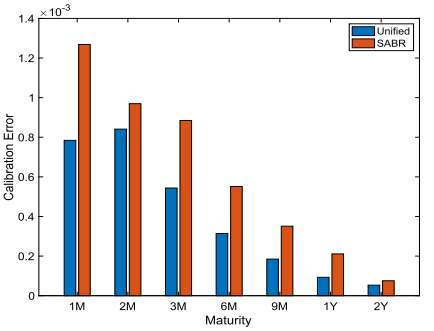

(h) Error between the market-implied volatility and the model-implied volatility

Fig. 5. Implied volatilities of the GBP/USD option, 3rd March, 2020 under the SABR and unified models and market-implied volatilities.

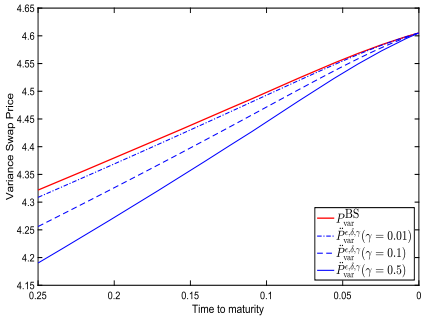

(a) P-function: $\epsilon = 0.1$

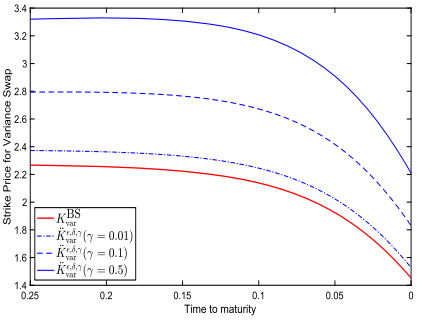

(b) Fair Strike Price: $\epsilon = 0.1$

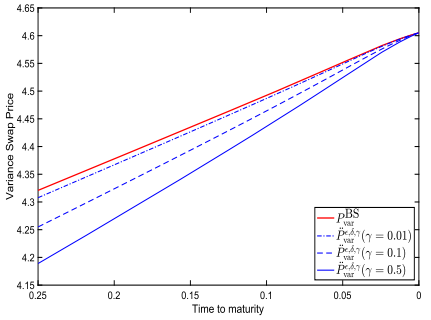

(c) P-function: $\epsilon = 0.05$

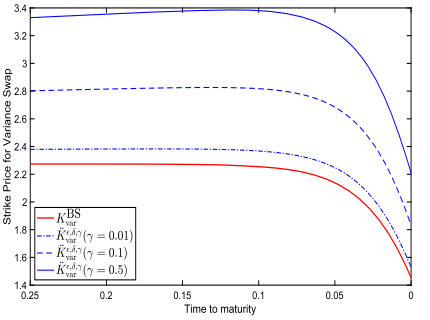

(d) Fair Strike Price: $\epsilon = 0.05$

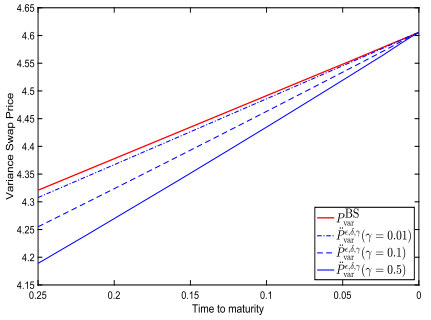

(e) P-function: $\epsilon = 0.01$

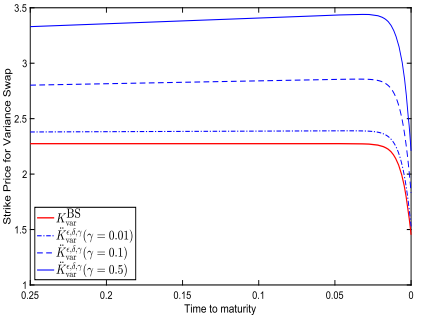

(f) Fair Strike Price: $\epsilon = 0.01$

Fig. 6. Comparison of the P-function and the fair strike price under the Black-Scholes model and the SABR-SVCEV model for various choices in the parameters ϵ and γ.

5. Conclusion

Both SABR and SVCEV models are the CEV based stochastic-local volatility models which have been used for many financial derivatives. This paper proposed a model unifying these two models and obtains an explicit valuation formula for the approximate derivative prices under the unified SABR-SVCEV model. The formula is expressed as a simple elegant form in terms of Mellin convolution, so that it requires only a single integral (instead of a double integral) calculation. The formula can be represented as the CEV price plus two perturbation terms related to the SABR and SVCEV related volatilities. Furthermore, we obtained a closed-form pricing formula that can be easily calculated using the well-known Black-Scholes derivative price in a reasonably practical situation for the elasticity of variance. This is a strong merit from a computational point of view. Two specific examples were provided to demonstrate the merits. We demonstrated the performance of the model in real-world scenarios using data from a foreign exchange option market.

As future work, one can modify the model introduced here in order to price American style derivatives or path-dependent exotic derivatives such as Asian, barrier and lookback options. In addition, the proposed model can be extended to capture more delicate features of volatilities such as fractional stochastic volatilities using the Malliavin calculus instead of the classical Itô calculus used in this paper.

Acknowledgements

The authors deeply thank the anonymous reviewers for the valuable comments and suggestions to improve this article. The work of S.-Y. Choi was supported by the National Research Foundation of Korea grant funded by the Korea government No.2021R1F1A1046138. The author J.-H. Kim thanks the financial support from the National Research Foundation of Korea under the grant number NRF2021R1A2C1004080.

Appendix A

For the proof of y independence of the terms P_{00}, P_{01} and P_{10} and the derivation of the PDEs in (2.9), the following lemmas are required. They are the solvability condition of a Poisson equation and the growth condition related to the operator $\mathcal{L}_0 = \alpha(y)\partial_y + \frac{1}{2}\beta^2(y)\partial_{yy}$, respectively. In this paper, we assume that every term P_{ij} is assumed to satisfy the growth condition in Lemma 5.2.

Lemma 5.1. *The Poisson equation*

$$\mathcal{L}_0 p(t,s,x,y) + q(t,s,x,y) = 0$$

has a solution $p(t,s,x,y)$ if and only if the function q is centered with respect to the invariant distribution Φ of the process Y, i.e.,

$$\langle q(t,s,x,\cdot)\rangle = 0.$$

Proof. This is a version of the Fredholm alternative. Refer to Section 3.2 in Fouque et al. [14]. □

Lemma 5.2. *Assume that equation $\mathcal{L}_0 p(t,s,x,y) = 0$ admits only solutions that do not grow as fast as*

$$\partial_y p(t,s,x,y) \sim e^{\int(-2\alpha)/\beta^2 dy}, \quad y \to \infty.$$

Then the solution p does not depend on the variable y.

Proof. Solving equation $\left(\alpha(y)\partial_y + \frac{1}{2}\beta^2(y)\partial_{yy}\right) p = 0$ directly leads to this result. □

Plugging the expansion (2.7) into the PDE (2.4), one can obtain

$$\begin{aligned} \mathcal{L}_0 P_{00} &= 0, \\ \mathcal{L}_0 P_{01} + \mathcal{L}_1 P_{00} &= 0, \\ \mathcal{L}_0 P_{02} + \mathcal{L}_1 P_{01} + \mathcal{L}_2 P_{00} &= 0, \\ \mathcal{L}_0 P_{03} + \mathcal{L}_1 P_{02} + \mathcal{L}_2 P_{01} &= 0. \end{aligned} \tag{A.1}$$

Then from the first equation in (A.1) we find that P_{00} is independent of y according to Lemma 5.2. This leads to $\mathcal{L}_0 P_{01} = 0$ from the second equation in (A.1) which again implies the y-independence of the term P_{01}. Then from the third equation in (A.1), we obtain

$$\langle \mathcal{L}_2 \rangle P_{00} = 0. \tag{A.2}$$

Applying $P_{02} = -\mathcal{L}_0^{-1}\mathcal{L}_2 P_{00}$ from the third equation in (A.1) to the fourth equation in (A.1) and using (A.2), we have

$$\langle \mathcal{L}_2 \rangle P_{01} = \langle \mathcal{L}_1 \mathcal{L}_0^{-1} \left(\mathcal{L}_2 - \langle \mathcal{L}_2 \rangle\right)\rangle P_{00} \tag{A.3}$$

by Lemma 5.1. Plugging the expansion (2.7) into the PDE (2.4), one also can obtain

$$\begin{aligned} \mathcal{L}_0 P_{10} &= 0, \\ \mathcal{L}_0 P_{11} + \mathcal{L}_1 P_{10} + \mathcal{M}_3 P_{00} &= 0, \\ \mathcal{L}_0 P_{12} + \mathcal{L}_1 P_{11} + \mathcal{L}_2 P_{10} + \mathcal{M}_3 P_{01} + \mathcal{M}_1 P_{00} &= 0. \end{aligned} \tag{A.4}$$

Then from (A.4) we find that P_{10} and P_{11} are y-independent by Lemma 5.2 and

$$\langle \mathcal{L}_2 \rangle P_{10} = -\langle \mathcal{M}_1 \rangle P_{00}, \tag{A.5}$$

by Lemma 5.1. Therefore, we have derived the PDEs (2.9) since (A.2), (A.3), and (A.5) obtained above are exactly the same as those PDEs.

Data availability

Data will be made available on request.

References

[1] P.S. Hagan, D. Kumar, A.S. Kesniewski, D.E. Woodward, Managing smile risk, Wilmott 1 (2002) 84–108.
[2] G. West, Calibration of the SABR model in illiquid markets, Appl. Math. Finance 12 (4) (2005) 371–385.
[3] P. Henry-Labordère, A general asymptotic implied volatility for stochastic volatility models, Available at SSRN, https://ssrn.com/abstract=698601, 2005.
[4] A. Antonov, M. Konikov, M. Spector, The free boundary SABR: natural extension to negative rates, Available at SSRN, https://ssrn.com/abstract=2557046, 2015.
[5] A. Van der Stoep, L.A. Grzelak, C.W. Oosterlee, The time-dependent FX-SABR model: efficient calibration based on effective parameters, Int. J. Theor. Appl. Finance 18 (6) (2015) 1550042.
[6] J. Guerrero, G. Orlando, Stochastic local volatility models and the Wei-Norman factorization method, Discrete Contin. Dyn. Syst. 15 (12) (2021) 3699–3722.
[7] Z. Cui, J.L. Kirkby, D. Nguyen, A general valuation framework for SABR and stochastic local volatility models, SIAM J. Financ. Math. 9 (2) (2018) 520–563.
[8] J. Cox, Notes on option pricing I: Constant elasticity of variance diffusions, Unpublished note Stanford University, 1975.
[9] J. Yu, On leverage in a stochastic volatility model, J. Econom. 127 (2005) 165–178.
[10] H. Geman, Y.F. Shih, Modeling commodity prices under the CEV model, J. Altern. Invest. 11 (3) (2009) 65–84.
[11] F. Black, M. Scholes, The Pricing of Options and Corporate Liabilities, J. Polit. Econ. 81 (3) (1973) 637–654, The University of Chicago Press.
[12] S.-Y. Choi, J.-P. Fouque, J.-H. Kim, Option pricing under hybrid stochastic and local volatility, Quant. Finance 13 (8) (2013) 1157–1165.
[13] J.-P. Fouque, G. Papanicolaou, R. Sircar, Mean-reverting stochastic volatility, Int. J. Theor. Appl. Finance 3 (1) (2000) 101–142.
[14] J.-P. Fouque, G. Papanicolaou, R. Sircar, K. Sølna, Multiscale Stochastic Volatility for Equity, Interest Rate, and Credit Derivatives, Cambridge University Press, 2011.
[15] R.Z. Khasminskii, On stochastic processes defined by differential equations with a small parameter, Theory Probab. Appl. 11 (1966) 211–228.
[16] G.C. Papanicolaou, W. Kohler, Asymptotic theory of mixing stochastic ordinary differential equations, Commun. Pure Appl. Math. 27 (5) (1974) 641–668.
[17] S. Cerrai, Khasminskii type averaging principle for stochastic reaction-diffusion equations, Ann. Appl. Probab. 19 (3) (2009) 899–948.
[18] J. Bao, Q. Song, G. Yin, C. Yuan, Ergodicity and strong limit results for two-time-scale functional stochastic differential equations, Stoch. Anal. Appl. 35 (6) (2017) 1030–1046.
[19] T.G. Bali, K.O. Demirtas, Testing mean reversion in financial market volatility: Evidence from S&P 500 index futures, J. Futures Mark. 28 (1) (2008) 1–33.
[20] D. Lee, Modeling commodity future price dynamics, 2022, ⟨hal-03758093⟩.
[21] P. Cotton, J.-P. Fouque, G. Papanicolaou, R. Sircar, Stochastic volatility corrections for interest rates derivatives, Math. Finance 14 (2004) 173–200.
[22] B. Hambly, N. Kolliopoulos, Fast mean-reversion asymptotics for large portfolios of stochastic volatility models, Finance Stoch. 24 (2020) 757–794.
[23] I. Karatzas, S. Shreve, Brownian Motion and Stochastic Calculus, 13, Springer Science & Business Media, 2012.
[24] L. Debnath, D. Bhatta, Integral Transforms and their Applications, CRC Press, Chapman & Hall, 2014.
[25] H.M. Srivastava, R.G. Buschman, Theory and Applications of Convolution Integral Equations, Kluwer Academic Publishers, Dordrecht, Boston and London, 1992.
[26] R.N. Bracewell, Fourier Transform and Its Applications, McGraw-Hill, 1999.
[27] J.-H. Yoon, J.-H. Kim, The pricing of vulnerable options with double Mellin transforms, J. Math. Anal. Appl. 422 (2015) 838–857.
[28] J.-H. Kim, J. Lee, S.-P. Zhu, S.-H. Yu, A multiscale correction to the Black–Scholes formula, Appl. Stoch. Models Bus. Ind. 30 (6) (2014) 753–765.
[29] R. Panini, R.P. Srivastav, Option pricing with Mellin transforms, Math. Comput. Model. 40 (2004) 43–56.
[30] R. Merton, Theory of rational option pricing, Bell J. Econ. Manag. Sci. 4 (1) (1973) 141–183.
[31] M. Broadie, A. Jain, The effect of jumps and discrete sampling on volatility and variance swaps, Int. J. Theor. Appl. Finance 11 (2008) 761–797.
[32] R. Jarrow, Y. Kchia, M. Larsson, P. Protter, Discretely sampled variance and volatility swaps versus their continuous approximations, Finance Stoch. 17 (2013) 305–324.
[33] D. Marquardt, An algorithm for least-squares estimation of nonlinear parameters, SIAM J. Appl. Math. 11 (2) (1963) 431–441.
[34] G.J. LeBeau, A parallel implementation of the direct simulation Monte Carlo method, Comput. Methods Appl. Mech. Eng. 174 (3–4) (1999) 319–337.
[35] E. Alerstam, T. Svensson, S. Andersson-Engels, Parallel computing with graphics processing units for high-speed Monte Carlo simulation of photon migration, J. Biomed. Opt. 13 (6) (2008) 060504.